

PURIFICATION OF ZIRCONIUM
BY
SOLID STATE ELECTROLYSIS
AND
ZONE REFINING

by

THOMAS TUCKER CLAUDSON

A THESIS

submitted to


OREGON STATE UNIVERSITY

in partial fulfillment of
the requirements for the
degree of


DOCTOR OF PHILOSOPHY

June 1962


APPROVED:




Professor of Mechanical Engineering
In Charge of Major



Head of Department of Mechanical Engineering



Chairman of School Graduate Committee



Dean of Graduate School

Date thesis is presented April 21, 1962

Typed by Lilah N. Potter

ACKNOWLEDGEMENTS

The author has always felt fortunate in being a student of Professor Olaf G. Paasche who was responsible in no small way for providing the inspiration and opportunity to obtain this graduate degree. This opportunity of expressing sincere appreciation for his teaching, help, and guidance in this work is greatly appreciated.

The help and guidance of Messrs. Haruo Kato, Gene Asai, and Monroe D. Carver is also greatly appreciated. Their suggestions were of considerable aid to the author in completing this thesis. The author wishes to express his thank you to the many others who have contributed their skills and time to this thesis.

Acknowledgement is especially made to the United States Department of Interior, Bureau of Mines, Albany, Oregon, under whose Fellowship Agreement with Oregon State University this work was made possible.

TABLE OF CONTENTS

	Page
INTRODUCTION.	1
THEORY OF ELECTROLYTIC TRANSPORT.	11
Solid State Electrolysis.	11
THEORY OF ZONE REFINING	20
Floating Zone Technique	20
TEST PROCEDURES	31
Material Preparation.	31
Equipment	32
Zone Refining Procedure	35
Solid State Electrolysis Procedure.	44
RESULTS OF INVESTIGATION.	47
Results of Zone Refining.	47
Results of Solid State Electrolysis	56
CONCLUSIONS	81
RECOMMENDATIONS	85
BIBLIOGRAPHY.	87
APPENDIX I.	91
APPENDIX II	95

LIST OF FIGURES

		Page
Figure 1	Location of Interstices in a Hexagonal Close-packed Structure of Zirconium (alpha phase).	6
2	Zirconium-Oxygen System.	8
3	14
4	22
5	Approximate Concentration of Solute After Passage of One Molten Zone Through a Charge of Uniform Mean Composition, C_o	25
6	Solid State Electrolysis Purification Apparatus.	36
7	Equipment Used in the Investigation of Zirconium Purification by Solid State Electrolysis and Zone Refining	37
8	Electron Beam Power Supply and Vacuum System Used for Zone Refining Zirconium	38
9	Traverse Mechanism and Current Concentrator Used in Zone Refining Zirconium	40
10	Current Concentrator Used in Zone Refining Zirconium Rods by Induction . .	41
11	Traverse Mechanism and Filament Assembly for Zone Refining Zirconium Rods by Electron Beam Melting.	43
12	Zirconium Rods after Zone Refining at 10, 5, and 2½ inches/hour for One, Two, and Three Passes.	48
13	Zirconium Rod After Zone Refining for Three Passes at 2½ inches/hour	49
14	Zirconium Rod After Zone Refining by Induction.	50
15	Zirconium Rod After Zone Refining by Electron Beam.	50

LIST OF FIGURES - Cont.

		Page
Figure 16	Photomicrographs Showing the Relative Impurity Content of Zirconium Rods after Zone Refining for One, Two, and Three Passes at 5 inches.	57
17	Photomicrographs Showing the Relative Impurity Content of Zirconium Rods after Zone Refining for One, Two, and Three Passes at 10 inches per hour.	58
18	Photomicrographs Showing the Relative Impurity Content of Zirconium Rods after Zone Refining for One, Two, and Three Passes at 2½ inches per hour.	59
19	Zirconium Rod After Having Undergone Solid State Electrolysis at 1800 C for 200 Hours	60
20	Oxygen Concentration Gradient Over Length of Zirconium Rod After Heating by Direct Current to 1800°C for 240 Hours	66
21	Photomicrographs Showing Microstructures of Zirconium Rods Being Held at 1800 C at 3 Volt Potential for (a) 213 Hours and (b) 70 Hours. .	75
22	Photomicrographs Showing Microstructure of Zirconium Rods After Being Held at 1800 C at 4 Volts Potential for (a) 24 Hours, (b) 110 Hours, and (c) 200 Hours.	76
23	Photomicrograph Showing Microstructure of Zirconium Rod Held at 1800 C for 240 Hours at 5 Volt Potential	78
24	Photomicrographs of a Zirconium Rod Held at 1800 C for 240 Hours Illustrating the Difference in Microstructure due to the Relative Oxygen Content at Mid-section and Anode. . .	79

LIST OF TABLES

	Page
Table 1 Impurity Analysis Comparison Between Iodide Crystal Bar Zirconium and Kroll Process Zirconium Material used in this Investigation.	32
2 Impurity Analysis of Zone Refined Zirconium Rods	53
3 Oxygen Analysis of Zirconium Rods Sub- mitted to Solid State Electrolysis . . .	64
4 Analysis of Oxygen Content Along the Length of Zirconium Rods Which Have Been Submitted to the Effects of Solid State Electrolysis for 240 Hours	65

PURIFICATION OF ZIRCONIUM
BY SOLID STATE ELECTROLYSIS
AND ZONE REFINING

INTRODUCTION

Zirconium metal was first isolated in laboratory quantities in 1824 by Berzeleus (1, p. 121-127). It was not until 1925 that the technology of zirconium made a significant advance due to the efforts of deBoer and Van Arkel who developed the basic iodide process for refining the metal. Metal produced in this manner was the first zirconium metal which exhibited good ductility and could be cold worked. It was recognized by these workers that impurities such as oxygen and nitrogen have a marked effect on the mechanical properties of zirconium especially in the reduction of ductility. Since that time improvements have been made on the iodide process as well as many new methods of producing ductile zirconium, i.e., bomb reduction of zirconium tetrachloride with sodium and magnesium reduction of zirconium tetrachloride commonly known as the Kroll process. All of these methods are designed to minimize the amount of oxygen and nitrogen contained in the metal. Efforts to purify zirconium further have continued to this day. It is the purpose of this project to investigate two possible methods of

purifying zirconium still further in order that its true properties can be determined more precisely and that its relationships in alloying with other metals will be more accurately known.

The impurity atoms exist in the parent metal in various forms depending upon the relative properties of the parent and impurity atoms. It is usual to classify the imperfections associated with some types of impurity atoms into three categories: atomic imperfections; line imperfections; and surface imperfections. Surface imperfections (grain boundaries, twin boundaries, etc.) and line imperfections (dislocations) do not, in general, exist in thermal equilibrium below the melting point of a solid and are usually metastable resulting from incidents of growth, mechanical deformation, or thermal history. Atomic imperfections, however, are characterized by the fact that they can exist in thermal equilibrium in a crystal. They consist usually of misplaced or missing atoms as in the case of lattice vacancies, substitutional impurities, and interstitial impurities.

The interstitial impurity is of primary importance to the investigations to be described here since this is the type of lattice imperfection associated most commonly to the hexagonal closed-packed crystal structure of zirconium. An interstitial atom is one occupying a position

in the lattice which is not normally occupied in a perfect crystal. An interstitial solution is formed then when the solute atoms are interspersed among the solvent atoms in the holes generated by the close packing of the solvent atoms. This type of solution, then, requires that the interstitial atoms be of small enough size to fit in their interstitial positions. In the face centered cubic and hexagonal close packed structures the ratio of the radius of an interstitial hole to the radius of an atom at a lattice point is about 0.41. This same ratio in the body centered cubic structure is 0.29 indicating a decreased tendency to form interstitial solutions. The elements H, C, N, B, and O are known to form such interstitial solutions, and their radii are all less than 1.0 Å.

The interstitial atom may be a normal atom of the crystal. We are, however, more interested in the case where a foreign atom (impurity atom such as oxygen) has taken a position in the lattice. From the atomic theory of structure of metals, the interstitial impurity atom can be thought of as being able to move from one site to a neighboring site through the crystal lattice. This fundamental idea will be of primary importance in the development of the theory of solid state electrolysis. We are fundamentally concerned with the oxygen impurity

in zirconium under the solid state electrolysis portion of this investigation since oxygen is the element which is greatly affected by this treatment and because of the great effect it has upon the properties of zirconium.

Zirconium has the hexagonal close-packed crystal structure in the alpha phase at temperatures to 862 C where it transforms into the beta phase and exists in the body centered cubic crystal structure. Because of size differences (atomic radius of O = 0.66 Å, atomic radius of Zr = 1.616 Å) oxygen atoms are considered to occupy octahedral positions. In a study of the structure of interstitial compounds with transition metals, it has been shown that if the size of the nonmetal is less than 0.59 of the metal atom, an interstitial structure is formed (10, p. 556). As a means of understanding the aspects of interstitial structures, the following characteristics are listed:

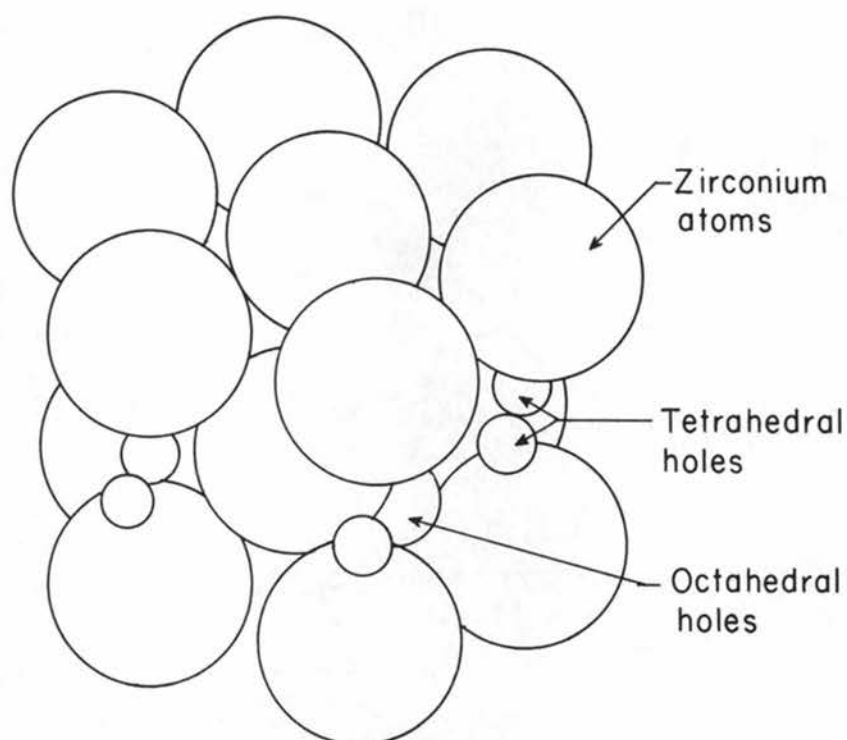
1. The metal atoms are assumed to be in contact and the structure is usually the same as, or very similar to, the metal structure.
2. The nonmetal atoms are situated in interstices between the metal atoms in such a way that the largest spaces are occupied. In this manner the maximum contact is maintained and maximum coordination is achieved.

3. A wide range of composition is possible within each phase.

It is well-known that oxygen is very soluble in zirconium and that the oxide formed is very stable to temperatures exceeding 2000 C. By means of a brief historical explanation, deBoer and Fast noted in 1936 that a zirconium wire with considerable oxide on its surface brightened upon heating in a vacuum. They studied the influence of oxygen on the alpha to beta transition and concluded that oxygen dissolved in the zirconium structure in large quantities without forming a new phase. An X-ray diffraction study showed that up to 29 atomic percent oxygen can be dissolved in alpha zirconium without a phase change (20, p. 558).

Results of these X-ray analyses and of other researches have shown that the specific gravity of this metal increases with absorption of oxygen. Also changes in the lattice cell dimensions are evident upon increasing the oxygen content. These facts lead to the conclusion that the oxygen atoms are absorbed in interstitial positions in the metal, probably in the octahedral positions as mentioned previously. Figure 1 shows the probable position of the interstitial atoms of oxygen in the zirconium structure.

The oxygen thus absorbed in the zirconium lattice



61-306

FIGURE 1.—Location of Interstices in a Hexagonal Close-packed Structure of Zirconium (alpha phase).

in solid solution is tightly bound as proven by the fact that the metal containing oxygen can be heated to the melting point (1852 C) or above without oxygen evolution. To illustrate the solubility of oxygen in zirconium the phase diagram for this system is shown in Figure 2. This shows that oxygen is soluble in zirconium to about 29 atomic percent. In this range there is no evidence of compounds such as ZrO or Zr_2O_3 . Above 29 atomic percent the compound ZrO_2 is in stable equilibrium with alpha zirconium. The crystal structure of ZrO_2 has been reported in four crystalline modifications: monoclinic; tetragonal; cubic; and hexagonal (20, p. 559). The monoclinic form is stable up to 1000 C, the tetragonal form to 1900 C, and the cubic form at higher temperatures. The hexagonal modification has been formed by long heating at 1900 C.

In recent years zirconium and its alloys have become very important materials used in the field of nuclear engineering. The use of zirconium stems primarily from its relatively good mechanical and chemical properties under varying reactor environments and from its low neutron cross section. Unalloyed zirconium was found to exhibit rather poor corrosion resistance to water under most reactor operating conditions. It became important then to study the alloys of zirconium to

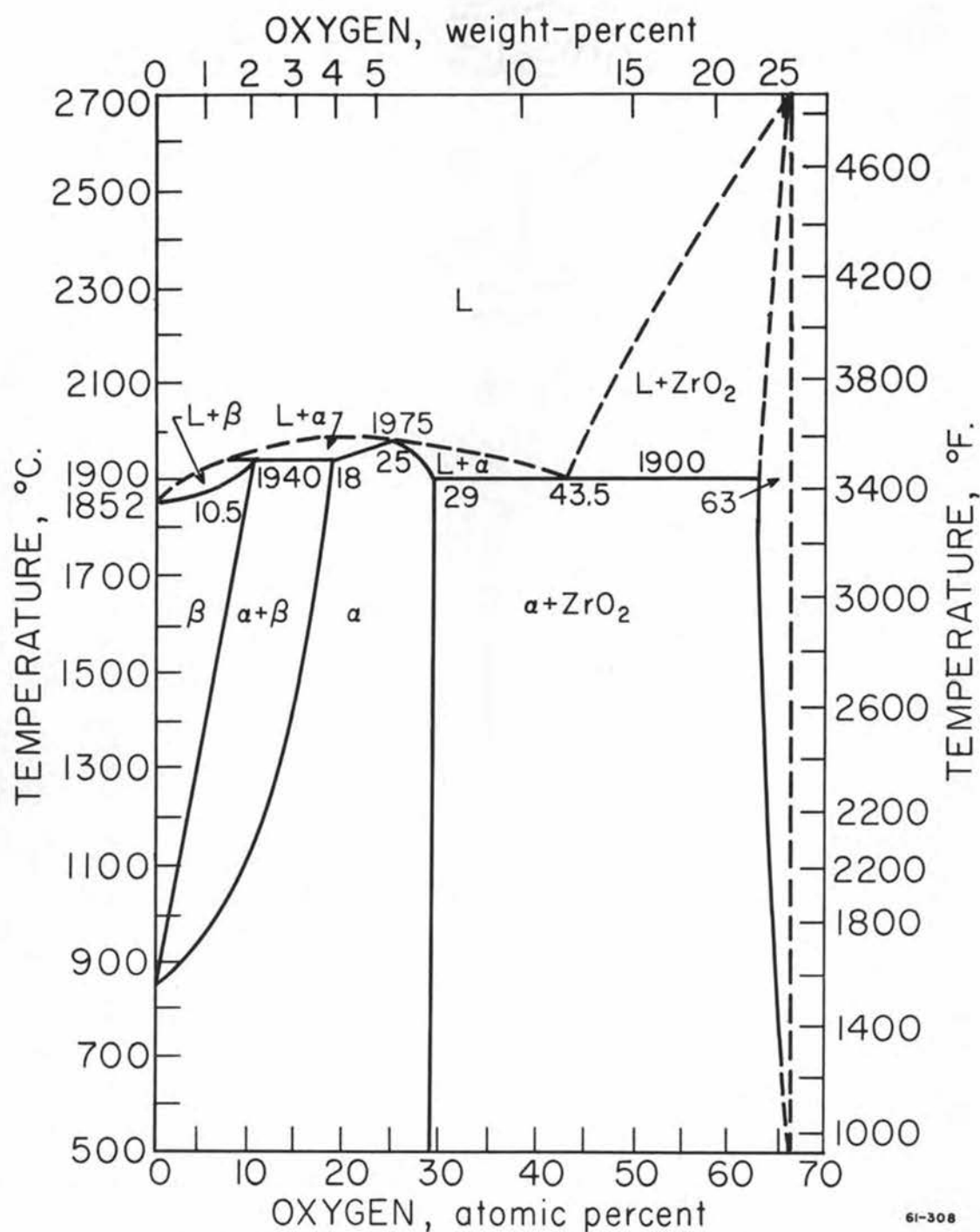


FIGURE 2—Zirconium-Oxygen System.
(Journal of Metals, AIME.)

find suitable material which would withstand all the environmental conditions found in reactor operations. This naturally led to the study of the phase diagrams of the various alloys of zirconium, especially those of the ZrFe, ZrCu, ZrNi, ZrMn, ZrSn, and ZrTi systems.

The accuracy with which a phase diagram can be determined depends, among other things, upon the purity of the base metals and upon the type and number of lattice imperfections. In the case of zirconium alloys it is particularly true that the amount of oxygen present can change the transformation temperature by several degrees. It is a well-known tendency of zirconium to dissolve oxygen at elevated temperatures rather than form an insoluble oxide. This tendency has dominated the preparation of alloys used in equilibrium diagram studies which involve more than 5 to 10 percent zirconium. For instance, the effect of oxygen on the alpha to beta transformation temperature of alpha zirconium is raised with increasing oxygen additions, and the transformation takes place over a range of temperatures, rather than at a single point. This was clearly demonstrated by deBoer and Fast in 1940. As an example, one percent oxygen raises the transformation temperature about 140 C. With these facts in mind, it is easy to understand that no phase diagram can be considered as final unless a

complete impurity analysis is given and that the elimination of impurities is essential in the determination of the true relationship between the metals to be alloyed.

THEORY OF ELECTROLYTIC TRANSPORT

Solid State Electrolysis

The first attempt to purify zirconium by means of solid state electrolysis was made in 1939 by deBoer and Fast (11, p. 161-167). They had earlier concluded from the influence of oxygen and nitrogen on the crystallographic transition from the hexagonal to the cubic lattice structure of zirconium that these elements could be absorbed in large quantities without a new phase being formed and that the oxygen and nitrogen were present in the metal lattice as a solid solution. Since that time no further attempts have been made to purify zirconium by this means.

Success in purification depends to a great extent upon the mobility of oxygen in the zirconium lattice. That the mobility of oxygen in zirconium is substantial under certain conditions can be seen from two facts. First, oxygen is absorbed by solid zirconium from either gaseous oxygen or from ZrO_2 at temperatures above 1000 C and leads to a homogeneous phase. Second, the resistance-temperature curves of zirconium wire containing oxygen coincide for rising and falling temperatures even in the transition region. This is due to the probable overlap of 4 electrons per atom of the

Brillouin zones. Since the c/a ratio increases with increased temperature, this overlap will also increase thus causing a decrease in the electrical resistivity of the metal with an increase in the atomic volume.

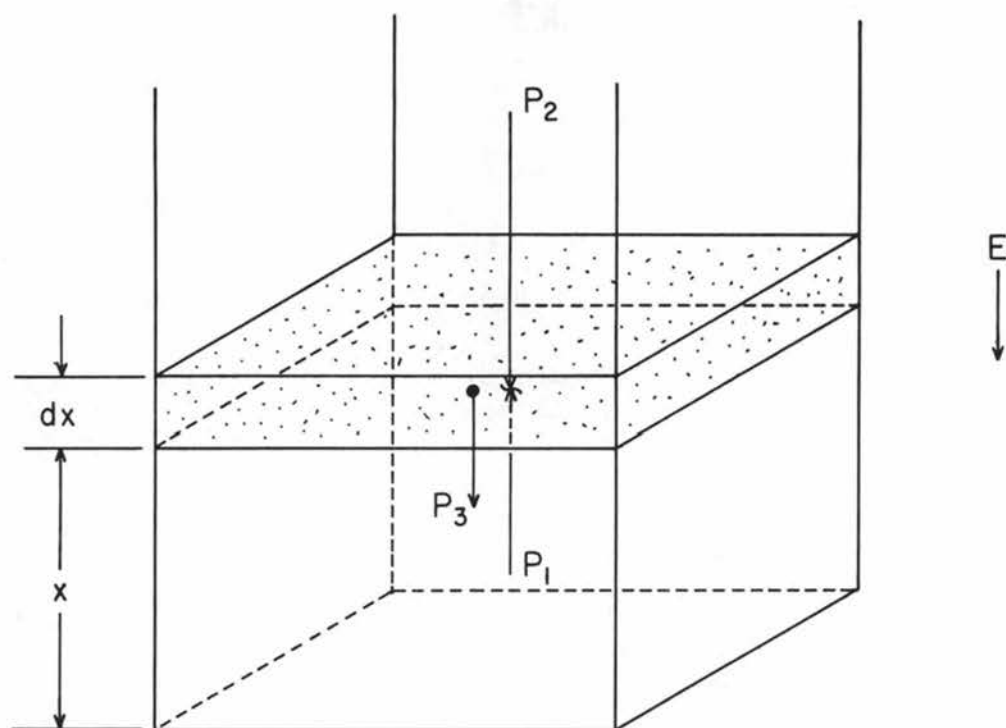
In an attempt to explain the migration phenomenon, it seems probable that if sufficient energy were given either an oxygen atom or a compound, such as ZrO_2 , the removal of an electron could be affected, thereby ionizing the particle. If then an electric field of sufficient strength were applied, the particle would migrate. The passage of a direct current through a metal or alloy results in a transport of matter as well as a flow of electrons. This phenomenon can be easily seen by accepting the fact that electric charges can be transported by ions as well as the electrons in metals and their alloys in an electric field. If the electric field is produced by direct current a preferential movement of atoms may occur. This general phenomenon has been under consideration and investigation since 1924 by Kremann, Schwarz, Seith, Jost, Wagner and their associates (14, p. 182-193). The transport of an atom through a metallic lattice depends mostly upon its mobility. The mobility, K , of an atom can be defined in general terms as the ratio of the average "drift" velocity to the intensity of the electric field. Since

there is a direct relationship between the mobility of an atom and its diffusion rate, a knowledge of the diffusion rates of the system under consideration is essential. Also, it is important to know the valency of the atoms under consideration.

In deriving the relationship between the mobility and the diffusion rate of an atom through a lattice under the influence of an electric field, one may obtain some basic relationships by considering a situation similar to that of the Boltzmann relationship. Consider a cloud of ions under the influence of a field of force and consider the forces on an elementary column of ions as in Figure 3. If the column of ions has a cross-sectional area of A square centimeters at constant temperature, free from all outside influences other than the electric field, and if x is the distance in centimeters measured in a direction opposite to that of the field, then one may write a simple force equilibrium equation. Let P_1 be the upward force due to a pressure p on the lower surface at x , let P_2 be a similar downward force at x , and let P_3 be a downward force due to the uniform field. Then one may write

$$P_1 - P_2 - P_3 = 0$$

or, for an area of A square centimeters



61-307

FIGURE 3

$$Ap(x) - Ap(x+dx) - AEnq(dx) = 0.$$

Rewriting this equation in terms of its partial derivative

$$Ap(x) - A\left[p(x) - \frac{\partial p}{\partial x}(dx)\right] - AnqE(dx) = 0$$

or,

$$-\frac{\partial p}{\partial x} + nqE = 0 \text{ -----(1)}$$

where,

E = field strength,

n = the number of ions per cubic centimeter,

and

q = the ionic charge.

Since $p = nkT$, we may write

$$-kT \frac{dn}{dx} + nqE = p'$$

where p' is now a force acting on a unit volume and $\frac{dn}{dx}$ is the concentration gradient which is equivalent in effect to an electric field since if the electric field is removed, the force of the equivalent field due to the concentration gradient will redistribute the ions. Let this equivalent field equal E' where

$$E' = -\frac{kT}{nq} \frac{dn}{dx} \text{ -----(2)}$$

Therefore, if a concentration gradient exists between any two points in a lattice, its equivalent electric

field results in an apparent potential difference between the points and will produce an identical ionic drift as an equivalent applied potential.

By definition of mobility we may write an expression for the average velocity of the ions as

$$u = K E \text{ -----}(3)$$

or, since we must include the effect of both the electric field, E , and the equivalent field, E' , we may write

$$u = K (E + E') .$$

Substituting for E' we obtain the following relation,

$$u = K \left(E - \frac{kT}{nq} \frac{dn}{dx} \right) \text{ -----}(4)$$

Furthermore, if it is assumed that the applied field E is removed, a diffusion current may be assumed to be present due to the motion of the ions under the influence of the concentration gradient. Multiplying the previous equation by n and letting $E = 0$, we obtain

$$nu = - \frac{KkT}{q} \frac{dn}{dx} .$$

By definition of the diffusion constant, D , the charge q may be expressed as

$$q = -D \frac{dn}{dx} = ne \text{ -----}(5)$$

and substituting this into the previous equation we obtain

$$\frac{D}{K} = \frac{kT}{e} \text{-----}(6)$$

which shows the relationship between the diffusion constant and the mobility of the diffusing ions.

As mentioned previously the transport of atoms through a metallic lattice depends largely upon the mobility of the atoms. A number called the transport number, t_i , is usually designated to describe this phenomena and is defined as the number of gram-atoms, n_i , of the component i which are transported by one Faraday, F . Therefore, by this definition

$$t_i = \frac{n_i F}{It'} = \frac{D_i C_i E_i F}{kTfJ} \text{-----}(7)$$

where, I = electric current, amperes

J = current density, amperes/square centimeter

t' = time, sec

C_i = concentration in gram atoms/cubic centimeter

D_i = rate of self diffusion of i

E_i = force due to the electric field strength.

The term f is a factor which takes into account the various possibilities of the ions jumping for both the vacancy and interstitial diffusion. If we rewrite t_i

in terms of the migration velocity u_i we may express the transport number as

$$t_i = \frac{u_i C_i F}{k'} \text{-----} (8)$$

where k' is a specific conductivity.

The above equations for the transport number are valid for the general case of an ion migrating through a metallic lattice. The general field force E_i must, however, be divided into two components, an atomic interaction force E_w and a field force E_f . We may write for the field force

$$E_f = zeE \text{-----} (9)$$

where ze = charge on the ion,

E = field strength.

The atomic interaction force E_w is proportional to eE . We may express this force as

$$E_w = ZeE \text{-----} (10)$$

where Ze = charge on the matrix ion.

Rewriting equation (7) we may obtain

$$t_i = \frac{D_i C_i F (Z_i - z_i) e E}{k T f J} \text{-----} (11)$$

Equation (11) describes satisfactorily the electrolytic transport of ions through a metallic lattice. It might be mentioned here that the sign and magnitude of Z_i as

compared to z_i determines the direction of transport of the migrating ion, a positive sign implying an interaction force towards the anode and a negative sign implying transport towards the cathode. Therefore, if an atom is to move towards the anode the quantity $(Z_i - z_i)$ must be positive.

Many hypotheses have been put forth since 1924 upon the transport theory of ions passing through a metallic lattice (14, p. 192). In recent years attempts through quantum mechanics have been made in order that a more true picture may be made to conform to the theories and practices of modern atomic theory.

H. B. Huntington in unpublished works has derived equations based upon the above basic concepts and using the additional resistance to migration imposed by lattice vacancies by quantum mechanical methods. His values have been in error by only one order of magnitude in comparison with experimental results accomplished by H. Wever (31, p. 283-290).

THEORY OF ZONE REFINING

Floating Zone Technique

The first paper published on zone melting was written by W. G. Pfann in 1952 (23, p. 1). Since that time over one hundred papers have been published describing various applications or modifications to the process originally developed for work in the then new semiconductor field. It was realized that zone melting could be applied to any crystalline substance capable of being melted which exhibits a difference in impurity concentration between the liquid and the freezing solid. In general, zone melting denotes a family of methods which control the distribution of soluble impurities or solutes in crystalline materials. The term zone refining is used to denote a zone melting technique of which the goal is to purify the substance under consideration.

To understand the purification process, it is necessary to analyze a molten zone traversing a rod. From the physical appearance of such a zone, the rod seems to have solid-liquid interfaces, one a freezing interface and the other a melting interface. It is primarily what happens at the freezing interface which determines the redistribution of impurities. At the

melting interface the material is melted and merely becomes a part of the molten zone. However, at the freezing interface the solute concentration in the material about to freeze differs, in general, from that in the liquid. Hence, the melting point of the solvent is either raised or lowered depending upon the solute concentration in the freezing solid. If the solute concentration is lower than the liquid, the melting point of the solvent is lowered, and the solute will be rejected by the freezing solid and will then accumulate in the liquid. Alternately, if the solute concentration in the freezing solid is greater than in the liquid, the solute raises the melting point of the solvent, and the liquid will then be depleted of the solute. Hence, the freezing interface determines the impurity content, and it can either reject or attract solutes depending on the solute material and its concentration.

One may more easily understand the purification process by using for an illustration a simple eutectic system with limited solubility. Such a system is shown in Figure 4. The basic parameters of zone refining consist of two fundamental types: first, those of the apparatus, such as zone length, ingot length, number of passes, and rate of travel; and second, the distribution coefficient, a parameter of the material, defined as the

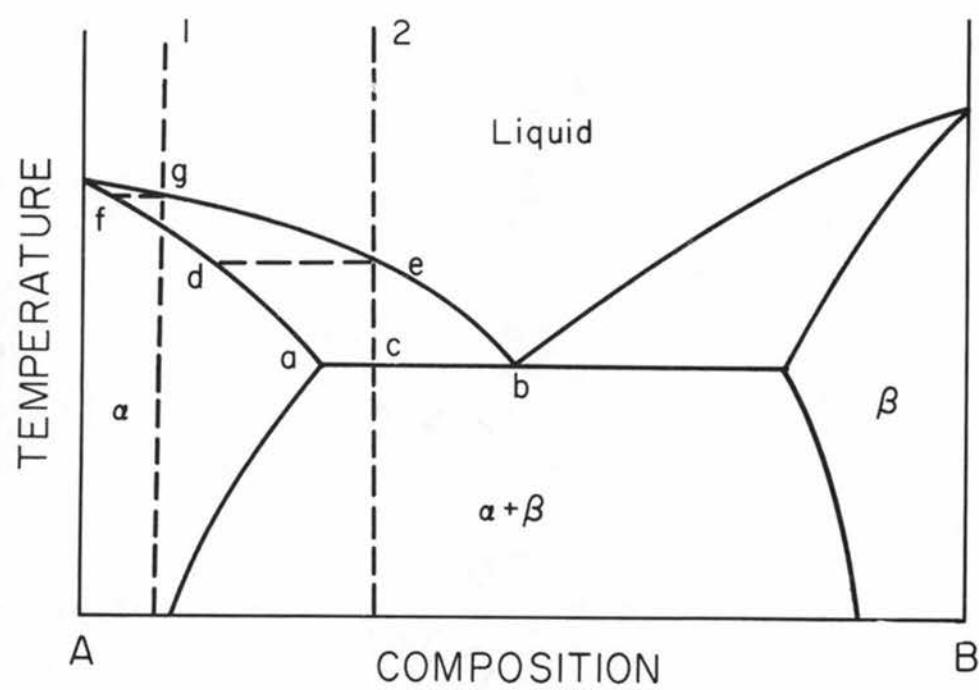


FIGURE 4

61-309

ratio of the solute concentration in the freezing solid to that in the main body of the liquid. This distribution coefficient is usually denoted by k and will be greater than unity if the solute raises the melting point of the solvent or less than unity if it lowers the melting point of the solvent.

Referring now to Figure 4, let us assume that an ingot of mean composition 1 is to be refined. As the zone begins to cool from the liquid range, a temperature g on the liquidus is attained. The alpha forming at this temperature will be of mean composition f . As the zone traverses the length of the specimen, the material being left behind in the solid state will be of this new mean composition. By repeating this process the material will be purified to a greater extent. Zone refining of an ingot of initial mean composition 2 is somewhat different. A small zone produced in the ingot is moved along the ingot at a constant rate. As the molten zone is moved along the ingot, a portion begins to freeze at a temperature indicated by e on Figure 4 with a resulting concentration d of alpha. With further travel of the zone the composition of the alpha reaches a as the composition of the zone reaches b , the eutectic composition. As the ingot travels further, the freezing of alternate layers of eutectic and alpha of composition a should appear

since the zone is constantly taking in solids of composition c . If thorough mixing of the zone occurs, the freezing out of alpha enriches the zone causing the freezing out of the eutectic which in turn freezes out the alpha since the eutectic was depleted out of the zone by its freezing. In this manner one may segregate the impurities, and thus purify the ingot.

Figure 5 illustrates the distribution of the solute after a single pass of the zone. As can be seen, the curve has three distinct regions and shows how the purification process occurs. When the zone width is first formed in the specimen, its concentration is that of the initial concentration of the melted material, C_0 . As the zone advances a short distance it freezes out at $x = 0$ a layer of solid of concentration kC_0 by melting. As a result the zone is enriched and subsequently freezes out the higher concentrations. As the zone progresses, enrichment continues at a decreasing rate until its concentration attains the value C_0/k . From this point on the concentration entering and leaving the zone are equal and the concentration in the freezing solid remains C_0 until the zone reaches the end of the specimen. For the last zone width as the heat source moves to the end of the specimen the zone width is decreased and causes the solute concentration to rise. From this curve one sees

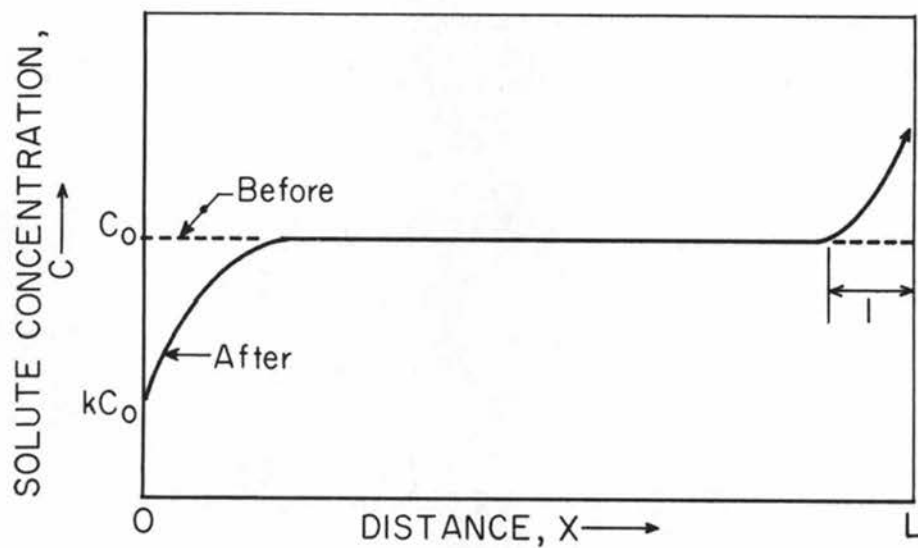


FIGURE 5.—Approximate Concentration of Solute After Passage of One Molten Zone Through a Charge of Uniform Mean Composition, C_0 .

61-319

that for a single pass the purification effect is initially at the beginning of the specimen. There follows a leveling process, and finally a higher impurity region is formed at the end of the specimen.

There have been developed several mathematical methods for describing the purification process which occurs in zone refining (23, p. 28-56). Equations developed have been too difficult to solve analytically and so various numerical methods have been used. For the purpose of this investigation a method following that of N. W. Lord was found to be most useful (19, p. 1531-1536).

In order to simplify the calculations, the following idealized conditions are assumed to exist:

(1) a constant length and cross sectional area of the zone produced; (2) a constant distribution coefficient as defined above; (3) an initially homogeneous composition of a binary alloy of zirconium; (4) no volume change when the molten zone freezes; and (5) no diffusion occurring in the solid portion of the rod.

It is of particular interest to estimate the concentration of an impurity atom after n passes of the zone over the rod. As above, we may define the distribution coefficient as

$$k = \frac{C_n(x)}{C_{nL}(x)} \text{-----(1)}$$

where $C_n(x)$ is the impurity concentration of a solid ingot at some distance x during the n^{th} pass of a molten zone and $C_{nL}(x)$ is the impurity concentration of a liquid zone from which the solid at distance x is formed.

The impurity concentration $C_n(x)$ can be determined from the analysis of what happens when new material is taken into the molten zone and of what happens when the material is ejected upon freezing. The amount of solute added during an incremental advance, dx , is due to the melting in of a solid portion $C_{n-1}(x) dx$ and the freezing out of $kC_{nL}(x)$. This difference may be expressed for an ingot of length d and of zone width l as,

$$l \frac{d}{dx} [C_{nL}(x)] dx = C_{n-1}(x+l) - kC_{nL}(x)$$

or in terms of $C_n(x)$

$$\frac{d}{dx} C_n(x) + \frac{k}{l} C_n(x) = \frac{k}{l} C_{n-1}(x+l) \text{-----(2)}$$

The solution of equation (2) is

$$C_n(x) = e^{-\frac{kx}{l}} \left[\int_0^x \frac{k}{l} C_{n-1}(x+l) e^{\frac{kx}{l}} dx + A \right] \text{----(3)}$$

For boundary conditions to evaluate the constant, A , we have that at the starting zone ($x = 0$), the total impurity content is constant. Therefore,

$$C_x(0) = C_{nL}(0) = \frac{1}{l} \int_0^l C_{n-1}(x) dx$$

or, substituting into equation (3) we may write the particular solution as

$$C_n(x) = \frac{k}{l} e^{-kx/l} \left[\int_0^x C_{n-1}(x+1) e^{kx/l} dx + \int_0^l C_{n-1}(x) dx \right] \text{-----}(4)$$

It will be convenient later to make the change of variable of x to a under the relationship of $x = al$. We may then rewrite equation (4) as

$$C_n(a) = k e^{-ka} \left[\int_0^a C_{n-1}(a+1) e^{ka} da + \int_0^l C_{n-1}(a) da \right] \text{-----}(5)$$

This last equation corresponds to the passage of a molten zone of unit length in units of a and the result is the concentration existing in the rod after the passage of the zone. If we let a single operation be

represented as θ in the equation equivalent to equation (5), then,

$$C_n(a) = \theta C_{n-1}(a). \text{-----}(6)$$

For repeated operations $\theta^{(r)}$ may be written in the following form,

$$C_n(a) = \theta^{(r)} C_{n-r}(a).$$

If we then make repeated operations on the term e^{-ka} we can express this as a finite sum of terms involving only a , k and the index of summation. Consider the effect of the first zone pass on a rod of uniform concentration, C_0 , then

$$C_1(a) = \theta C_0 = k e^{-ka} \left[\int_0^a C_0 e^{ka} da + \int_0^l C_0 da \right] \text{---}(7)$$

or, for a repeated operation

$$C_n(a) = C_{n-1}(a) - (1-k) C_0 \theta^{(n-1)} e^{-ka} \text{-----}(8)$$

which in terms of the differences in the concentration is

$$\frac{C_n(a) - C_{n+1}(a)}{C_{n-1}(a) - C_n(a)} = \frac{\theta^{(n)} e^{-ka}}{\theta^{(n-1)} e^{-ka}} \cdot \text{-----} (9)$$

Lord has published tables showing the first seven passes of a zone passing over a rod of uniform concentration which indicates the following general relationship

$$\frac{\theta^n e^{-ka}}{e^{-ka}} = \frac{\theta^{n-1} e^{-ka}}{e^{-ka}} - k^{n-1} e^{-nk} \left[\sum_{r=0}^{n-1} f_r^{(n)} a^r \right. \\ \left. (r+1-k) \right]$$

where, $f_r^{(n)} = \frac{n^{n-r-2}}{(n-r-1)!r!} \cdot$

Solutions of this general relationship can then be made to draw curves which will enable one to estimate the concentration of a rod specimen after any number of passes.

TEST PROCEDURES

Material Preparation

The material used for this investigation was obtained from the zirconium stores located at the U. S. Bureau of Mines in Albany, Oregon. Two types of zirconium were used, Westinghouse iodide crystal bar zirconium and commercial Kroll process ductile zirconium. The basic differences between these materials lie in the relative impurity content as shown in Table I.

Both materials were prepared for this investigation in the same manner. Ingots five inches in diameter and about eight inches in length were formed from bundles of zirconium by consumable electrode arc melting under a pressure of about 2×10^{-2} mm of Hg. The ingots were then machined free of surface voids and cracks and reduced to a diameter of $1\frac{1}{2}$ inches by press forging at a temperature of 850 C. Further reductions were made by swaging at 850 C. At frequent intervals between the stages of swaging, the rods were cleaned of scale by centerless grinding to avoid oxide contamination in the metal. Zirconium rods 0.250, 0.188, and 0.125 inches in diameter were obtained by this process. They were subsequently cut into lengths of about ten inches and cleaned by chemical etching.

TABLE I

Impurity Analysis Comparison
Between Iodide Crystal Bar Zirconium
and Kroll Process Zirconium Material
used in this Investigation

Impurity Element	Impurity Content-ppm	
	Iodide Zirconium	Kroll Process
O	300	1300
Al	450	90
Fe	260	600
Cu	20	20
Cr	20	80
Si	40	130
Mg	50	100
Ti	30	25
Ni	50	12
Sn	60	10

Equipment

The two methods chosen for study required two types of equipment. First, due to the high rate of reactivity which zirconium has with hydrogen, nitrogen, and oxygen, it was necessary and essential that all work for both methods be carried out under a high vacuum. Second, although both methods required heating the rod

specimens, the methods of heating for zone refining must, of course, be different from those of the electrolysis because of the theory behind each method.

The effect of solid state electrolysis appears only in the application of a direct current field. For this reason the power to heat the rod specimen was provided by a selenium rectifier d.c. power supply capable of producing 500 amperes at 24 volts. This power supply, manufactured by Rapid Electric Company, was controlled by a Rapidtrol oil submerged motor driven infinite variable transformer and operated from a 440 volt a.c. source. The stability of this power supply was excellent, operating well within the 3-5% power variation of the station input voltage.

Zone refining of zirconium requires that some method be provided by which a localized area of the rod may be heated to its melting point. Due to the high reactivity which zirconium exhibits, a floating zone is used to avoid contamination from crucibles. This usually entails the use of an induction coil or in recent years the use of a source of electrons properly accelerated and focused on the specimen. First attempts to zone refine zirconium were made using a 7.5 kw output induction unit operating at about 300 kc manufactured by Scientific Electric Company. It was found that this unit did not

provide sufficient control to produce a zone refined rod of uniform diameter. It was therefore necessary to use an existing electron beam zone refining furnace. The power source for this furnace was manufactured by Electro-Glass Laboratories and was designed to operate at a maximum beam power of 7.5 kw or 5000 volts at 1.5 amperes beam current. This apparatus provided sufficient power and control to produce with fair consistency rods of uniform diameter.

The vacuum chamber used in both methods consisted of an 18 inch diameter bell jar approximately 30 inches in height utilizing a standard "L" gasket to effect a vacuum seal to a polished base plate. The vacuum pumps were a Consolidated Vacuum Corporation 6 inch oil diffusion pump with a Kinney KC 15 c.f.m. roughing pump used also as the fore pump for the diffusion pump. A baffle was made and placed inside the transition collar located between the base plate and the toggle operated 6 inch Veeco high vacuum valve. Sufficient holes were drilled in the base plate to allow for insertion of electrical feed-throughs, water coolant lines, and auxiliary electrical feed-throughs.

It was calculated that a maximum current of 500 amperes would be required to heat the rods to temperature for the solid state electrolysis portion of this

investigation. For this reason 3/4 inch copper bus bars were fabricated and connected to standard commercial electrical feed-throughs. Connected to the bus bars were water cooled copper specimen holders through which current flowed to heat the zirconium rods. Since the rod was to be heated from room temperature to 1800 C, some means of allowing for thermal expansion was required. This was provided by designing and fabricating a telescoping sliding contact type of copper conductor used as the bottom (cathode) specimen holder. Figures 6, 7, and 8 show the equipment used for these tests.

Temperature measurements were made by using a standard optical pyrometer manufactured by Leeds and Northrup Company and calibrated by a Shaw two-color optical pyrometer. Accuracy of the measurements was ± 5 C at 1800 C.

Zone Refining Procedure

As previously mentioned, zone refining of a solid material is accomplished by causing a molten zone in the material to traverse the length of the specimen. This may be effected in two basic ways: either move the specimen through a stationary heating source or move the heating source past a stationary specimen. In this investigation the first method was used.

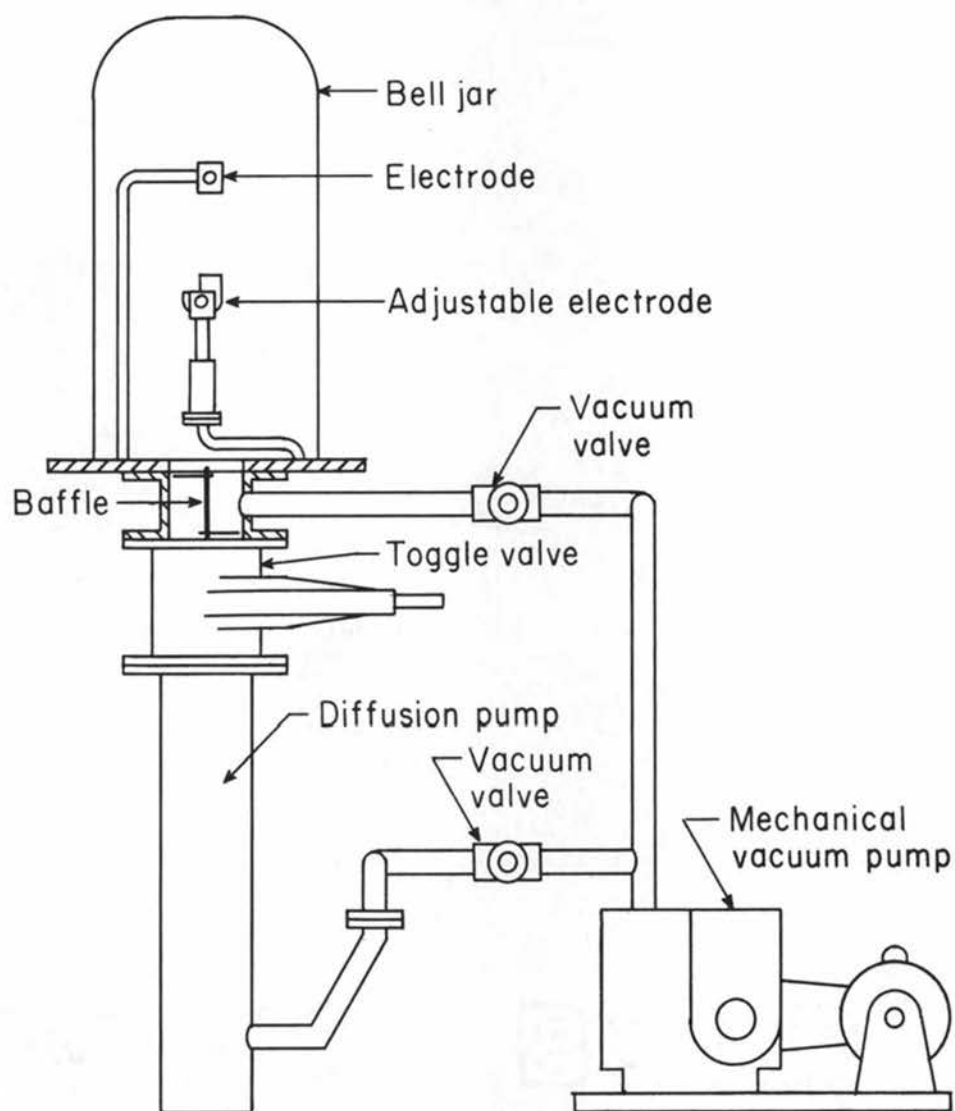


FIGURE 6.—Solid State Electrolysis Purification Apparatus.

61-305



FIGURE 7. -- Equipment Used in the Investigation of Zirconium Purification by Solid State Electrolysis and Zone Refining.



FIGURE 8. -- Electron Beam Power Supply and Vacuum System Used for Zone Refining Zirconium.

First attempts to zone refine zirconium in this investigation used $\frac{1}{4}$ inch diameter rods attached to a traverse mechanism driven by a threaded drive rod as shown in Figure 9. The threaded rod was rotated through a $\frac{1}{2}$ inch rotary vacuum seal by means of a stepless variable speed transmission. In this way any rate of travel could be used in refining the specimen.

The method of producing a narrow molten zone in the specimen posed a special problem due to the inadequacy of the existing induction heating unit. Sufficient coupling could not be attained using an induction coil of a single turn. Multiple turn coils produced a zone much too wide to be of use in this application. A current concentrator was therefore designed and fabricated. The device used is shown in Figure 10. An induction coil of nine coils was placed around the current concentrator as shown in Figure 9. The field from this coil was then concentrated around the $\frac{1}{2}$ inch diameter hole in the device due to the insulating air gap located between the water connections in the side of the apparatus. This concentrated field then had sufficient density to produce a molten zone about $\frac{3}{16}$ inch wide in the zirconium rod.

A second method was used in producing a narrow molten zone in the specimen. By means of an electron

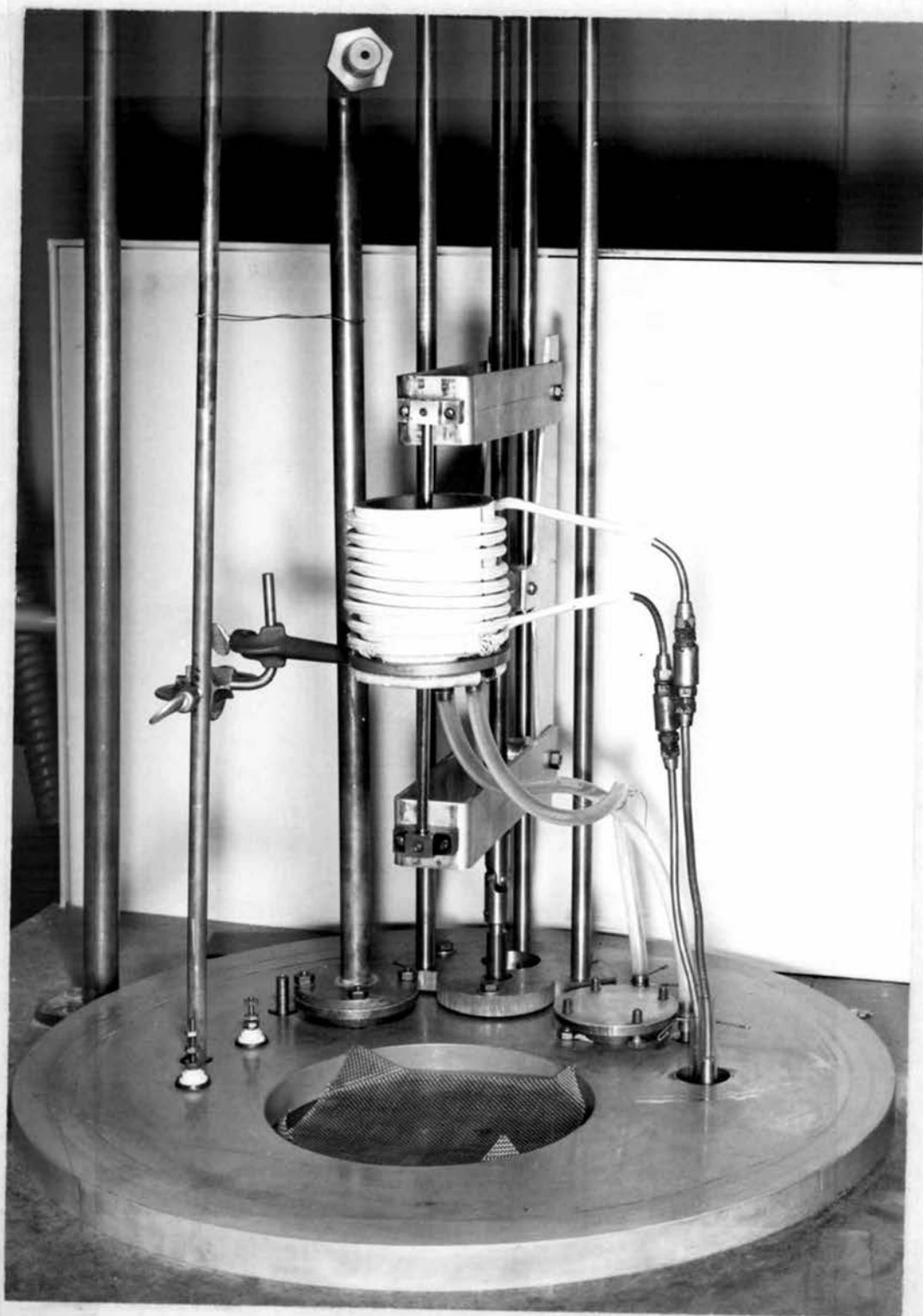


FIGURE 9. -- Traverse Mechanism and Current Concentrator Used in Zone Refining Zirconium.



FIGURE 10. -- Current Concentrator Used in Zone Refining Zirconium Rods by Induction.

beam produced from electrons emitted from a heated tungsten filament and accelerated by means of an electric potential of 3300 volts, a molten zone about 3/16 inch wide was produced. This means of heating proved to be the better of the two methods since more control could be obtained from the electron beam power supply. The filament support and traverse mechanism used are shown in Figure 11. The filament used in this operation was fabricated by forming a tungsten ribbon filament 1/16 inch wide and 0.025 inch thick into a semicircle and welding two such elements into a circle. Electrons flowing from such a surface travel approximately normal from the surface, thus acting also as a focusing device.

A series of nine zone refining runs were made varying the rate of travel of the specimen through the heating element and also the number of passes. Rates of travel of 10, 5, and 2½ inches per hour were made in passing the zone over the rod one, two, and three times at each rate. For each run the rod specimen was placed in the traverse mechanism in two sections as seen in Figure 11 and the bell jar evacuated to about 8×10^{-5} mm Hg pressure. A weld was then made at the junction of the two pieces of zirconium and a length of three to five inches zone refined. By welding the two rods together any stress or misalignment due to thermal

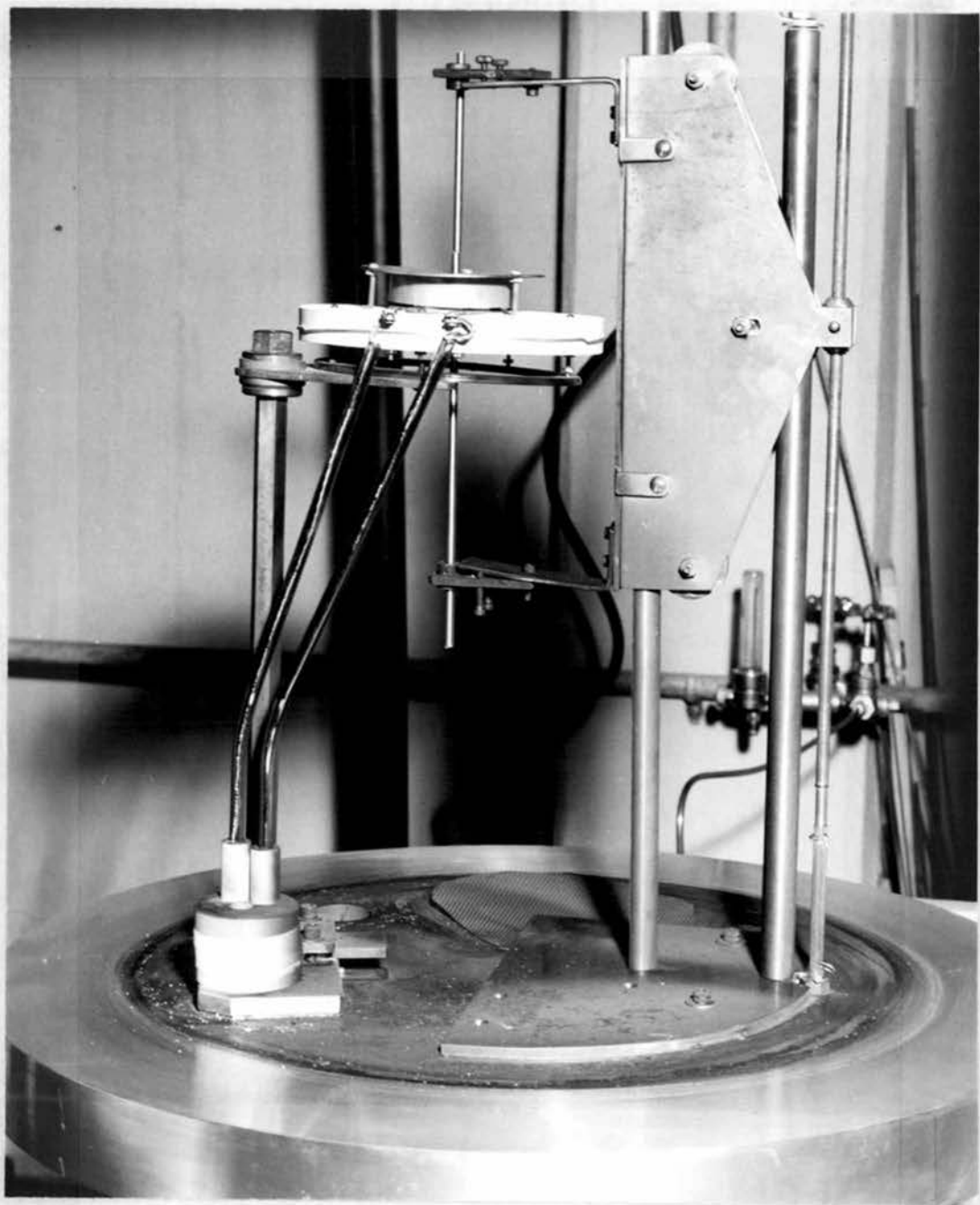


FIGURE 11. -- Traverse Mechanism and Filament Assembly
for Zone Refining Zirconium Rods by
Electron Beam Melting.

expansion of the metal upon heating was eliminated. After zone refining the rods were removed, cleaned by chemically etching in a solution of 45 ml HNO_3 , 45 ml H_2O , and 10 ml HF, known commercially as B etch. Two samples from each rod, approximately 2 grams each, were taken from the center and last portion of the specimen for chemical analysis. Since impurities are supposedly swept along the rod as the zone progresses a comparison between the two analyses should show the effect of the purification process.

Solid State Electrolysis Procedure

Utilizing the equipment described previously, procedures were developed to show the effects of electrolysis upon solid zirconium rods. Since the mobility of atoms is a function of their temperature and since the migration rate is dependent upon the mobility, it was thought that by keeping the specimens at as high a temperature as possible and still maintain a solid state the migration of oxygen atoms would occur at the maximum rate possible. For this reason all specimens used in this investigation were maintained at a temperature of 1800 C.

For this series of tests, zirconium rods were placed between two water cooled electrodes and surrounded

by a cylindrical heat shield fabricated from zirconium sheet. The zirconium heat shield served two purposes. First, because at equilibrium its temperature was about 1200 C, it acted as an excellent gettering material to absorb impurities in the system. Second, it was necessary to use such a shield to keep the glass bell jar at a safe operating temperature. After assembling the rod and heat shield, the bell jar was closed and evacuated to a pressure of about 3×10^{-5} mm of Hg. The rod was then heated by its own resistance to a temperature of 1800 C by a direct current power supply.

Three series of tests were carried out using the above procedure. Each series of tests was run at a different potential difference for varying lengths of time up to 240 hours. This effected a variation of driving force upon the migration of the oxygen atoms. The variation in potential difference was made possible by using three different diameter rods as test specimens. In this way the three series of tests were run at 3, 4, and 5 volts potential for rods of 1/4, 3/16, and 1/8 inch diameter, respectively. The rods were ten inches in length, thus allowing about eight inches of test material which could be used for chemical and metallurgical analysis.

At the end of each test run, the power supply was turned off and the sample allowed to cool in the evacuated bell jar. A period of 30 minutes was allowed for cooling before air was admitted to the system and the rods removed. There was, then, no possibility of the specimens absorbing oxygen due to exposure to the atmosphere.

RESULTS OF INVESTIGATION

Results of Zone Refining

Figures 12 and 13 show several zirconium rods after zone refining by electron beam melting. The resulting rods were more uniform in diameter over the zone refined length as compared to rods previously zone refined by induction heating as seen in Figure 14. It was determined by experimental means that the non-uniform diameter was due to insufficient temperature control by the induction heating unit. It was not possible using this method to maintain the correct temperature in the zone which, when overheated, lessened the surface tension on the zone resulting in the non-uniform diameter. The lowered surface tension allows the molten zone to flow out causing a non-uniform diameter. Rods with the same type of imperfection could be produced by purposely overheating the zone with the electron beam.

It was found during the course of this investigation that the uniformity of diameter of a zone refined rod was also greatly dependent upon the design and fabrication of the electron beam filament. Several different diameter and configurations of filaments were tried. A circular filament $1\frac{1}{4}$ inches in diameter was found to produce the most satisfactory results. Filaments which

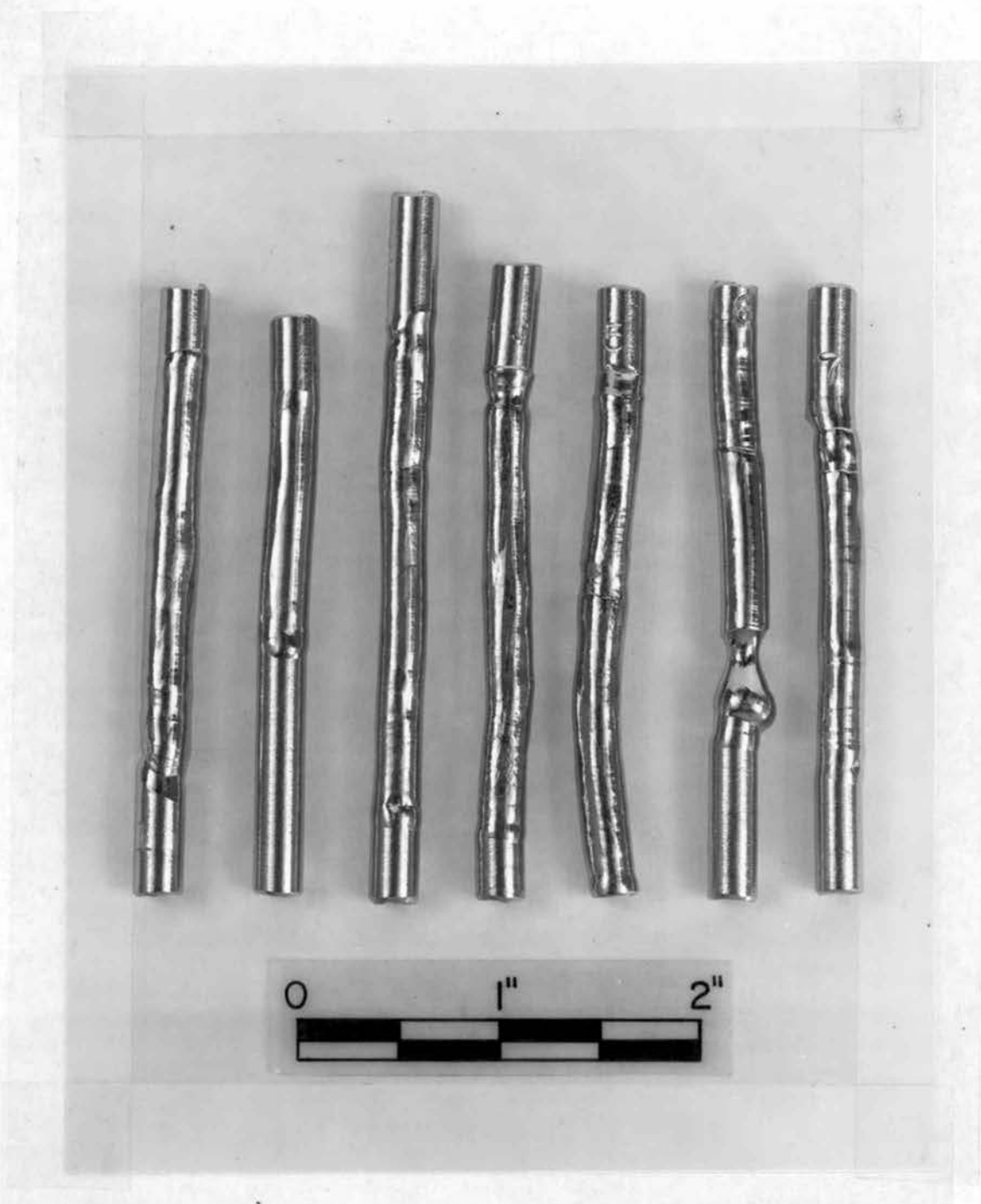


FIGURE 12. -- Zirconium Rods after Zone Refining at 10, 5, and 2½ inches/hour for One, Two, and Three Passes.

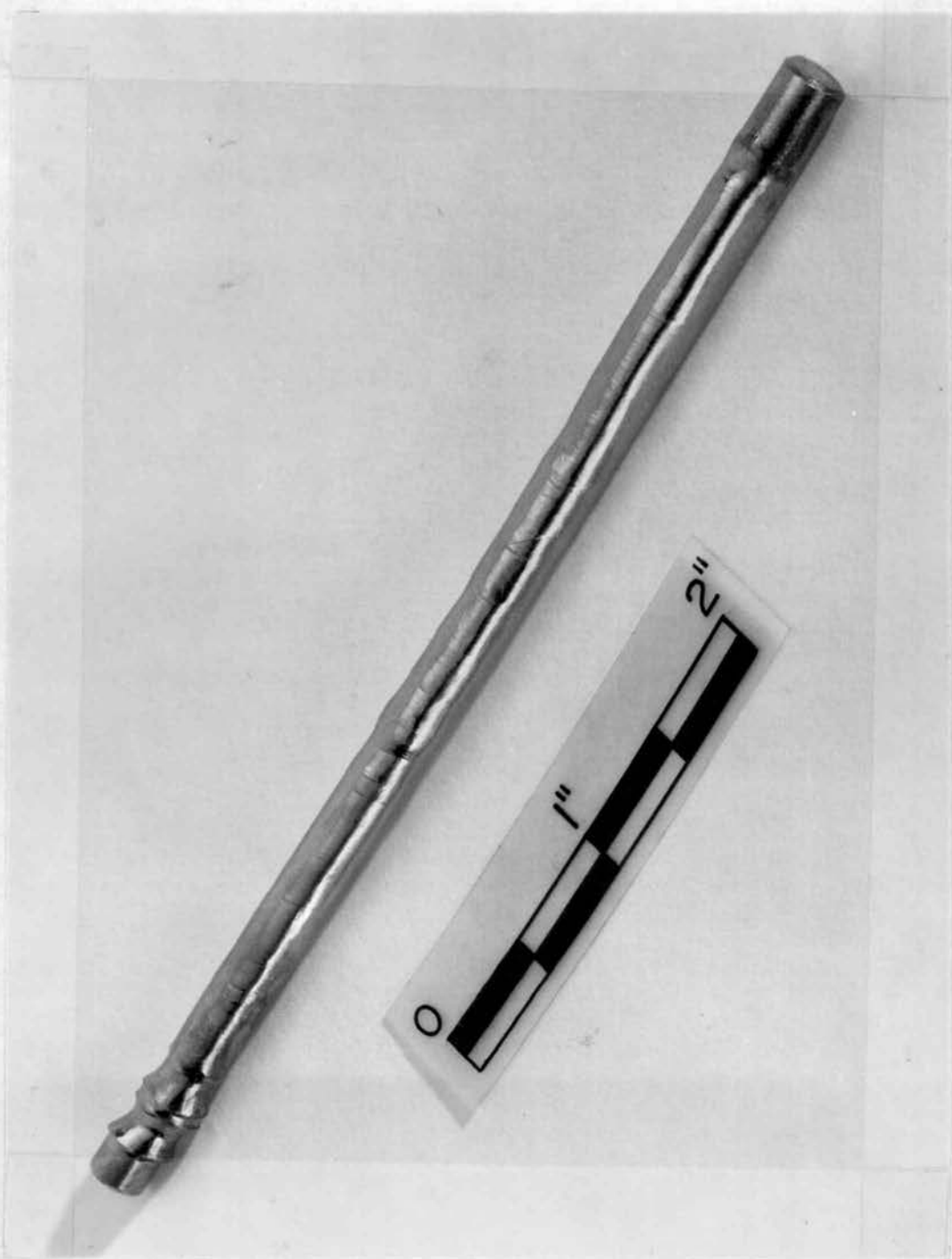


FIGURE 13. -- Zirconium Rod After Zone Refining for Three Passes at $2\frac{1}{2}$ inches/hour.

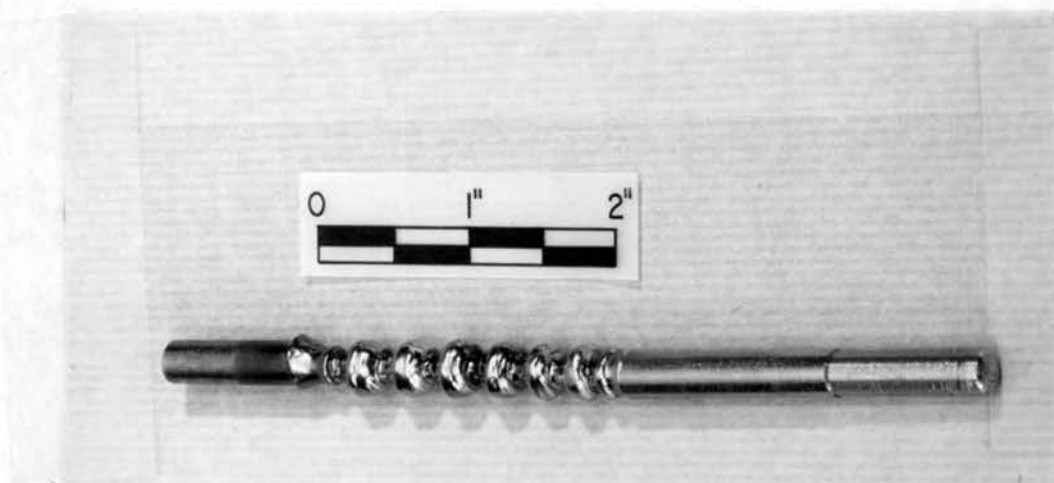


FIGURE 14. -- Zirconium Rod After Zone Refining by Induction. This shows the effect of overheating during the refining process.

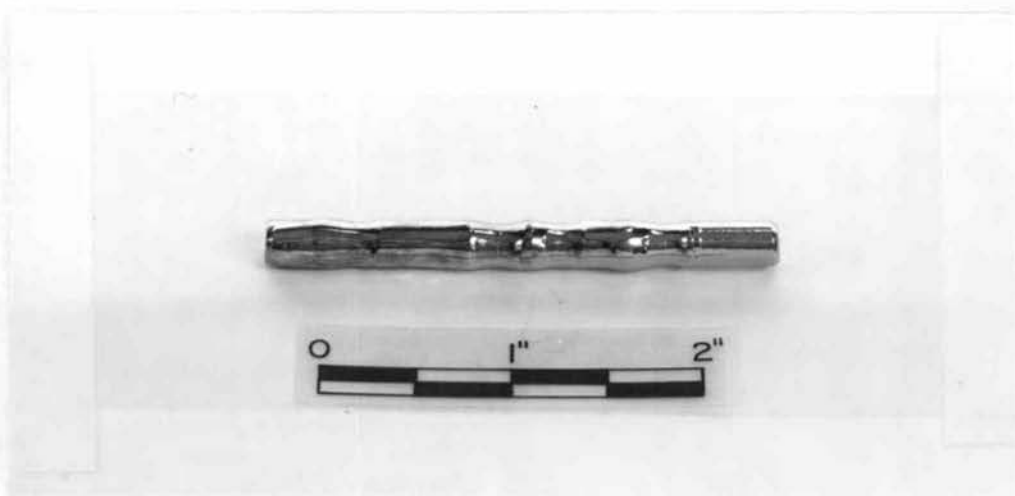


FIGURE 15. -- Zirconium Rod After Zone Refining by Electron Beam. This shows the effect of a non-uniform beam causing an incomplete zone through the diameter of the rod.

were not concentric around the rod or were warped due to being strained produced an uneven heating zone which either did not produce a uniform zone or did not melt completely through the rod diameter. Figure 15 shows a specimen produced from such a filament.

Two gram specimens were analyzed by chemical means by the Technical Services Branch of the U. S. Bureau of Mines, Albany, Oregon. Because of the low impurity content, special analytical procedures were developed.

The method used to analyze these zone refined specimens consisted basically in placing the zirconium specimens into HClO_4 and HF and evaporating the solution twice to remove all the HF. Sensitive reagents were then used to separate the iron, nickel, copper, and aluminum impurities into organic solutions and quantitative results obtained spectrophotometrically. These methods of analysis are accurate to within plus or minus one part per million over the range of sensitivity for which the analyses are valid. Using the above described procedures detection of Fe, Ni, Cu, and Al can be obtained to a lower limit of 0.05 ppm, 0.02 ppm, 0.05 ppm, and 0.2 ppm, respectively. An upper limit of detection of 60 ppm was found for the case of iron.

It must be emphasized at this point that it is very difficult to detect and analyze quantitatively for the impurity contents in the extremely low impurity levels which were obtained in this investigation. An industry wide problem has been the accurate analysis of impurities in low concentration by chemical means. Other methods such as measurements of resistivity have been used successfully in some instances. As will be mentioned later, some efforts to measure the resistivity of specimens containing various amounts of oxygen were made for this investigation but met with only minor success due primarily to the lack of electrical circuits stable enough to detect small changes in resistivity.

Table II shows the results of these chemical analyses. Determinations of the impurity levels of iron, copper, nickel, and aluminum after zone refining at rates of travel of 10, 5, and 2½ inches per hour for one, two, and three passes over the specimen are shown. These data show that, in general, a marked decrease in impurity level of the constituents was achieved. For example, in the case of a rod zone refined three times at a rate of 2½ inches per hour, the iron content was reduced to 1 ppm from an initial content of 600 ppm, copper to <0.05 ppm from 20 ppm, nickel to 1.8 ppm from 12 ppm, and aluminum to 3.3 ppm from 90 ppm. There are,

TABLE II

Impurity Analysis of Zone Refined Zirconium Rods

Rate of Travel inches/hour	Number of Passes	Fe		Cu		Ni		Al	
		mid	end	mid	end	mid	end	mid	end
10	1	1.6	0.8	3.7	3.1	7.9	10	<10	<10
10	2	33.5	29.7	0.86	4.52	28	75	3	4
10	3	26.8	29.2	1.14	2.78	79	57	5	4
5	1	1.2	0.4	<.05	<.05	6.0	9.0	<10	<10
5	2	14.8	20.8	<.05	1.71	90	>100	3	5
5	3	18.8	20.6	<.05	0.75	36	53	3	2
2½	1	24.1	30.7	<.05	52	2.8	30	3	1
2½	2	16.5	28.6	<.05	1.11	1.1	63	<1	<1
2½	3	1.0	25.3	<.05	1.11	1.8	3.3	*	1.0

*This sample was lost in the process of spectrophotometric measurement.

however, some serious discrepancies shown in these data when one compares the runs made at 10 inches per hour and 5 inches per hour. In both cases, after a single pass over the rod, chemical analysis indicates a greater degree of purification than after multiple passes. Also, some data indicate the rod to be more pure at the end of the zone refined region than in the center. Both of these results are contrary to the theory previously described.

These results can be explained by considering the rates of travel of the zone along the rod. At the more rapid rates of travel, time for segregation of impurities was not allowed. The decrease in the impurity level indicated by the analysis was then due primarily to the vaporization of the impurities since at the melting temperature of zirconium, 1852 C, the vapor pressure of iron, nickel, copper and aluminum is above the operating pressure of the vacuum system. In addition, it was mentioned previously that a new chemical analysis procedure was developed in order to detect the lower levels of impurities realized in this investigation. It was reported by the analyst that there was some difficulty in reproducing results from one run to another. This was believed to be due to the extreme sensitivity of the reagents used picking up impurities from the different

glassware, water, and chemicals used for each run. Because of this the quantitative results of the analyses may not show accurately the true relative impurity levels of the specimen. As will be described later, metallographic investigation of the specimen indicates results agreeing more with the theory of zone refining.

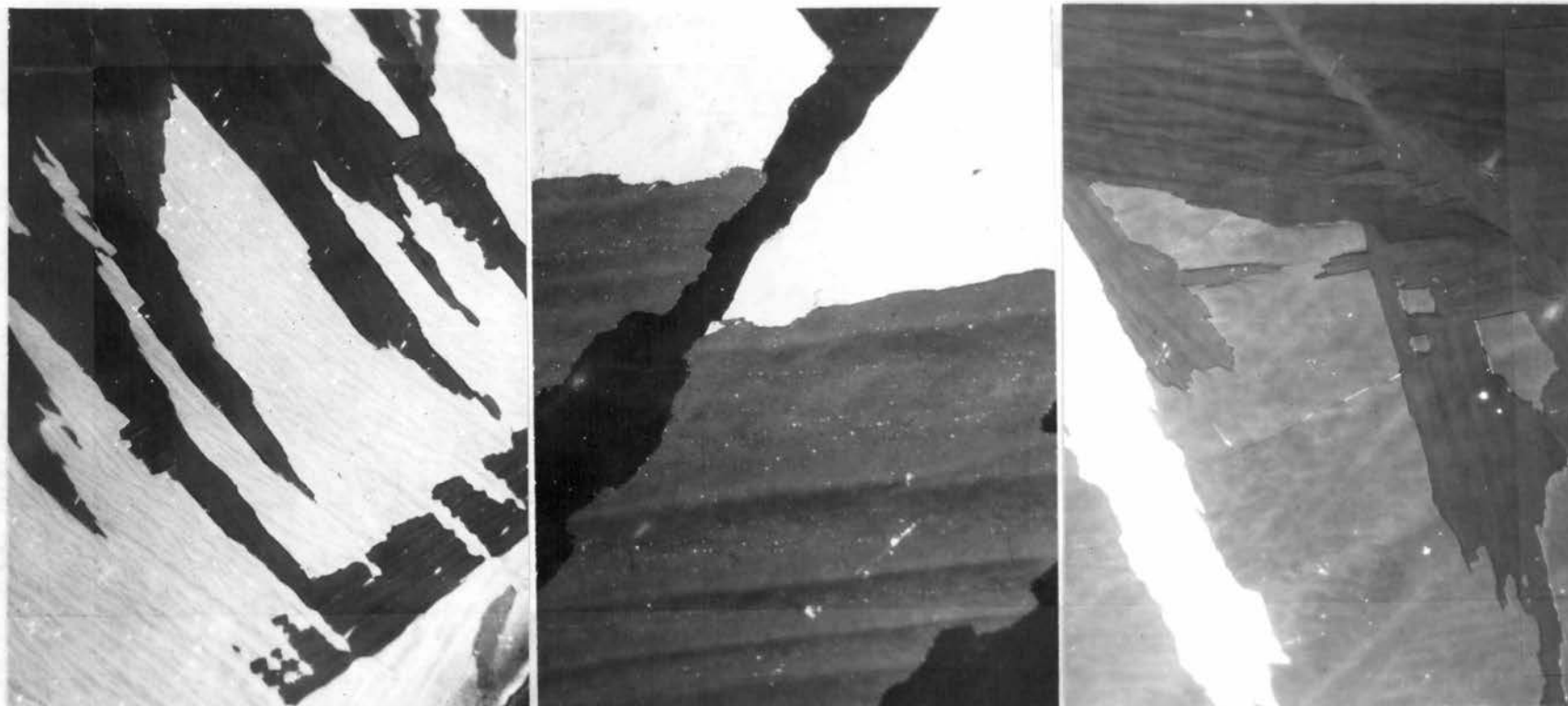
The analyses of specimens zone refined at $2\frac{1}{2}$ inches per hour indicate that sufficient time for impurity segregation was allowed. In this case data indicated that for the case of iron the impurity level was reduced from 600 ppm to 24.1 ppm, 16.5 ppm, and 1 ppm for one, two, and three passes, respectively. This, of course, agrees with the theory in that more impurities were removed with an increase of the number of passes. Similar results are shown for the other impurities for which analyses were made. Evidence from other investigators zone refining similar material indicates that good results from zone refining occurs only at the slower rates of travel. This work has, in general, indicated that good segregation of impurities occurred only at rates of travel less than one inch per hour in zone refining titanium metal.

Further evidence of purification can be seen in a metallographic study of the specimens taken at the middle sections of the zone refined rods. These

specimens were mounted in bakelite and polished mechanically under light pressure so as to avoid disturbing the appearance of the grain structure. After polishing the grain structure was made visible by means of chemical etching as previously described. Figures 16, 17, and 18 show the photomicrographs of the grain structure for each of the test conditions under polarized light at a magnification of 150 X. Under polarized light the impurities show up as white spots on the photomicrograph. By comparing the three photomicrographs on each figure there is evidence that the impurity level is reduced as the number of passes is increased at each of the three rates of travel. Moreover, by comparing each of the figures there is also evidence of a large decrease in impurity level for various rates of travel for one, two, and three passes. For example, there is a marked difference in the microstructure of a rod zone refined once at 10 inches per hour and a rod zone refined three times at 2½ inches per hour. In the latter case, the grains are much larger and are almost completely free of the evidence of impurities.

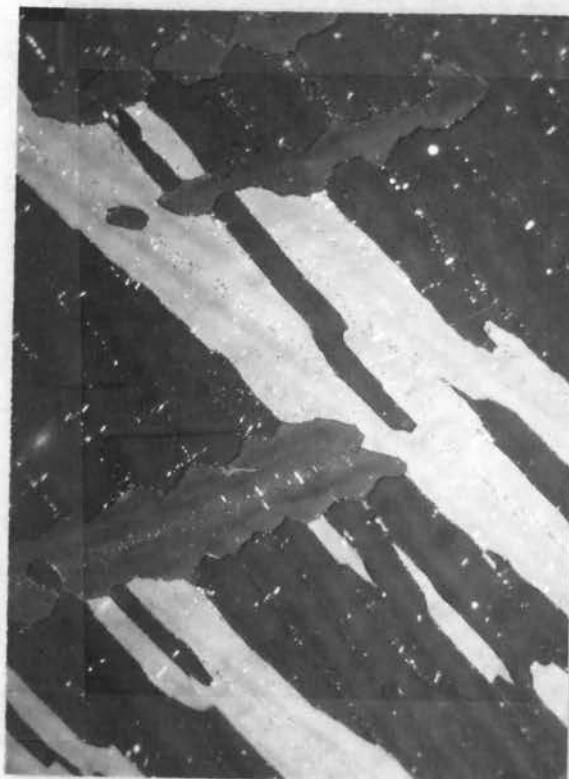
Results of Solid State Electrolysis

Figure 19 shows a typical zirconium rod after purification by solid state electrolysis. After a time



One pass at 5 inches/hour Two passes at 5 inches/hour Three passes at
5 inches/hour

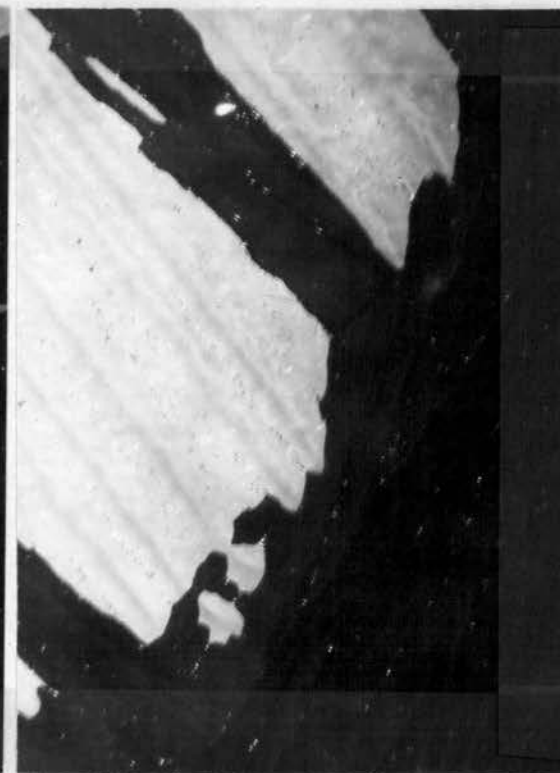
FIGURE 16. -- Photomicrographs Showing the Relative Impurity Content of Zirconium Rods after Zone Refining for One, Two, and Three Passes at 5 inches. Polarized light, B etch, 150X.



One pass at 10 inches/hour

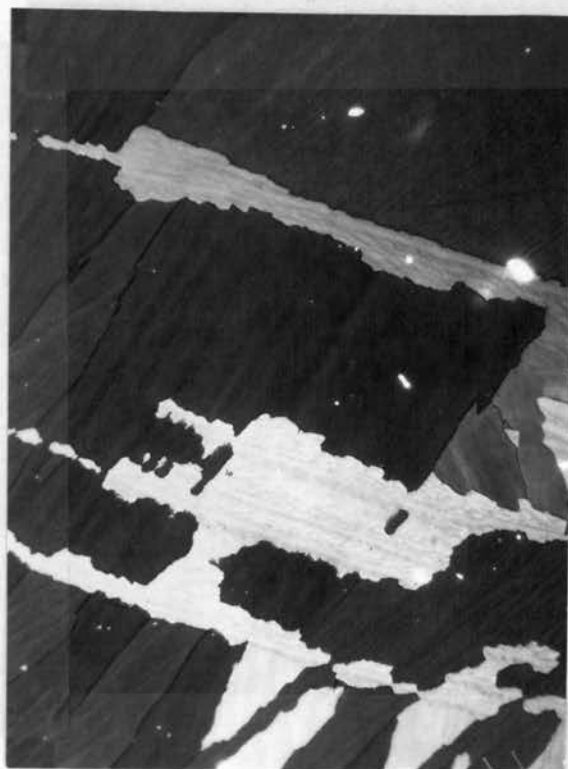


Two passes at 10 inches/hour

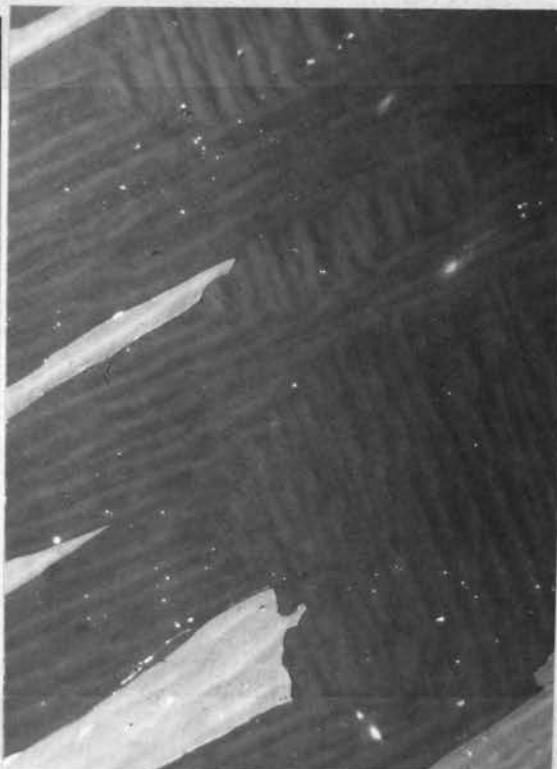


Three passes at
10 inches/hour

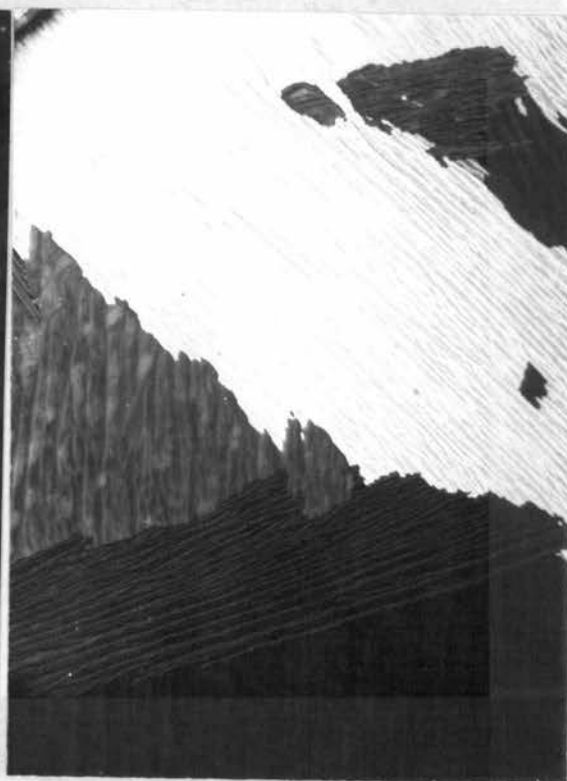
FIGURE 17. -- Photomicrographs Showing the Relative Impurity Content of Zirconium Rods after Zone Refining for One, Two, and Three Passes at 10 inches per hour. Polarized light, B etch, 150X.



One pass at $2\frac{1}{2}$ inches/hour



Two passes at $2\frac{1}{2}$ inches/hour



Three passes at
 $2\frac{1}{2}$ inches/hour

FIGURE 18. -- Photomicrographs showing the Relative Impurity Content of Zirconium Rods after Zone Refining for One, Two, and Three Passes at $2\frac{1}{2}$ inches per hour. Polarized light, B etch, 150X.

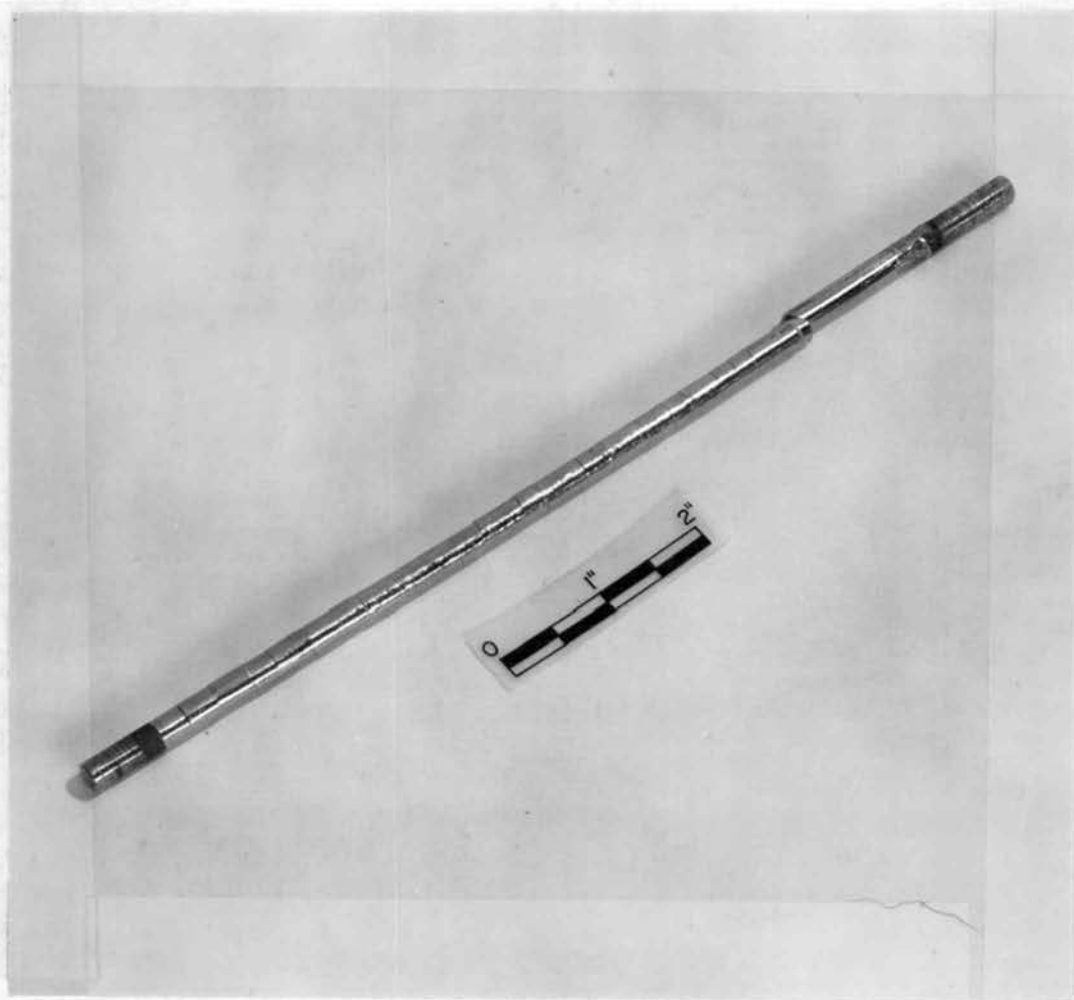


FIGURE 19. -- Zirconium Rod After Having Undergone Solid State Electrolysis at 1800 C for 200 Hours.

interval of 213 hours at 1800 C, the rod has retained its original luster but has developed a segmented appearance. Metallographic examination showed this segmentation to be due to large beta grain growth at the elevated temperature, the grain boundaries of which were retained upon cooling. It was at first thought that single crystals might have been formed, but both metallographic and X-ray analysis showed this not to be the case. It was found that extremely large and oriented grains had been formed. Also, it can be noticed that slipping has occurred near the cathode end of the rod. This type of behavior was observed in every case in the same location of the specimen. Since the rod was initially in tension before heating, the slipping must be due to the weight of the rod material above the slipping region because of its low strength at 1800 C.

After each test run the rods were removed from the electrodes. At this point it was evident that the mechanical properties of some rods were not uniform over the length of the rod. In nearly every case these rods could be easily broken at the anode end of the rod next to the electrode while remaining ductile at the cathode. One gram specimens were removed from the rod at various positions along the length of the rod by careful cutting to avoid overheating of the zirconium. These specimens

were then analyzed for oxygen by the Technical Services Branch of the U. S. Bureau of Mines.

The oxygen analysis was accomplished by means of the Leco gas analysis procedure. This is a commercially well known method of analysis now common in most laboratories and affords a relatively simple method of accurately determining the oxygen content in zirconium. The procedure starts with a solid sample of known weight, heated in pure argon with platinum and purified graphite. A solid solution of zirconium, platinum, and carbon is formed and carbon monoxide formed according to the following reaction,



The carbon monoxide coming off as a gas is then bubbled through a catalyst and leaves as carbon dioxide according to the following reaction,



The resulting carbon dioxide is then bubbled through a solution of barium hydroxide, and a change of electrical conductivity is measured and compared to a standard. The resulting measurement is then compared with a standard curve of oxygen content versus resistance which determines the amount of oxygen in the zirconium. Because

insufficient standards were available, no limit of accuracy could be assigned to the results of these analyses.

Table III lists the results of the oxygen analyses for the series of tests completed over a period of various lengths of time and at three, four, and five volts potential. It can be seen that the oxygen content is higher at the anode end of the rods than in the center. Also, if one examines the analyses of the rods run at a three volt potential, it is evident that little if any migration has taken place. It is only at a four volt potential and above that a significant amount of oxygen migration occurs.

Samples were analyzed at various intervals along rods run at a five volt potential and the results of those analyses are given in Table IV. These results show that there is a heavy concentration of oxygen at the anode end of the rod near the electrode and that this concentration decreases along the length of the rod toward the cathode. Figure 20 shows a curve of oxygen content as it is distributed along the length of the rod. The average initial oxygen impurity level in the rods was 1100 ppm. After purification the average oxygen level is seen to be 365 ppm or a decrease of about 70 percent.

TABLE III

Oxygen Analysis of Zirconium Rods
Submitted to Solid State Electrolysis

Time of Run Hours	Oxygen Content-ppm Anode	Middle	Rod Potential Volts
240	4,150	550	5
240	>4,000*	190	5
240	36,000	1,140	5
213	510	360	3
200	2,720	490	4
188	750	590	5
172	16,000	1,020	5
111	500	540	3
110	810	430	4
96	290	270	5
70	440	240	3
48	560	330	3
46	560	260	4
24	300	280	3
24	200	250	4
24	290	270	5

*The polarity of this run was opposite to that of the other runs. The sample for chemical analysis was lost due to its extreme brittleness and the oxygen result is an estimate.

TABLE IV

Analysis of Oxygen Content Along the Length
of Zirconium Rods Which Have Been Submitted
to the Effects of Solid State Electrolysis
for 240 Hours

Sample Number	Distance from Anode inches	Oxygen Content ppm
18	0	16,000
	0.5	1,340
	2.125	1,030
	3.375	1,020
	4.875	1,150
	7.000	1,100
19	0	36,000
	1.125	1,780
	2.25	1,290
	3.375	1,350
	5.875	1,140
20	0	4,000
	0.25	1,870
	0.75	830
	1.32	310
	3.25	260
	5.00	190
	7.75	190
21	0	4,150
	0.25	2,050
	2.70	520
	4.25	550
	6.00	540
	7.63	540

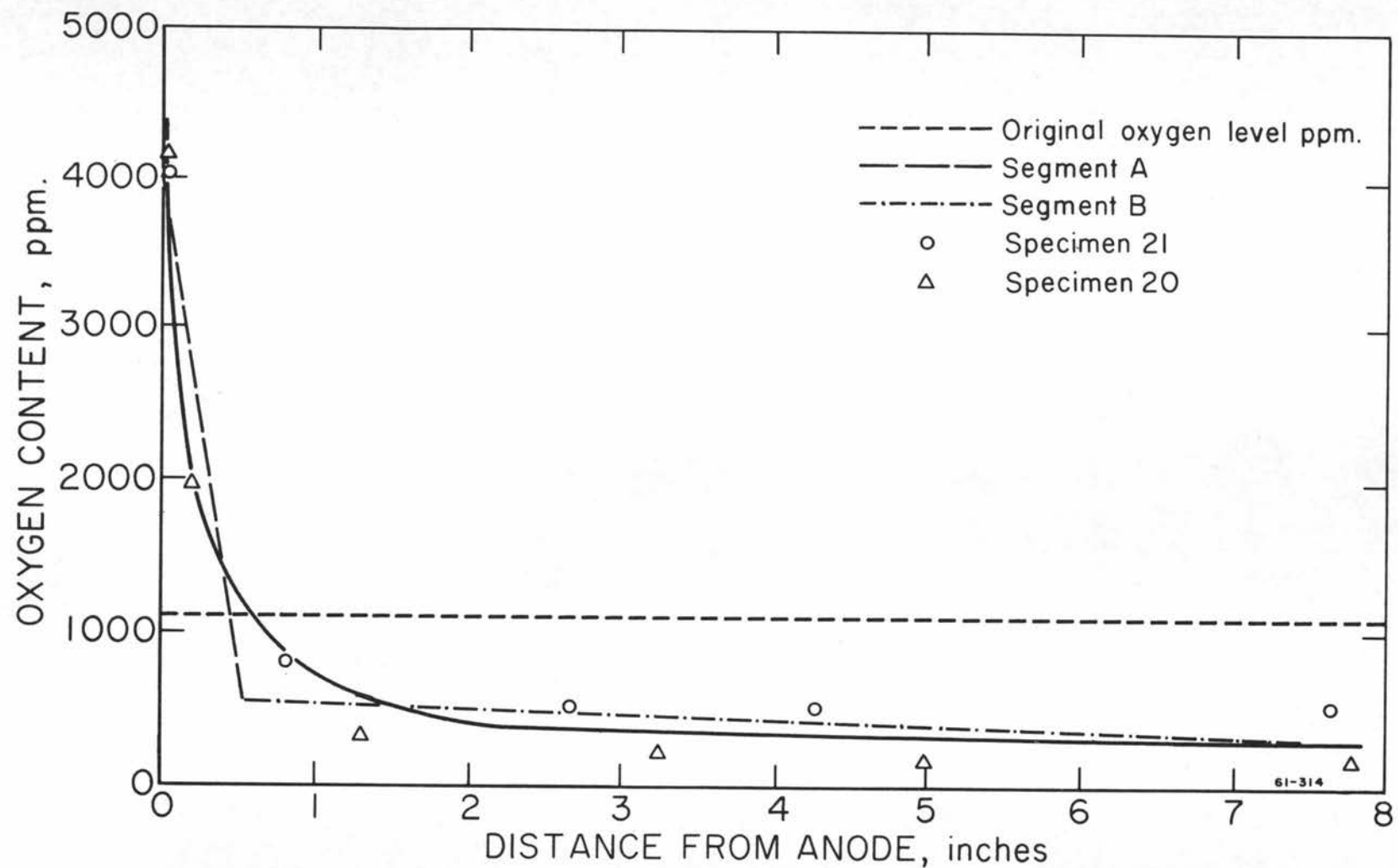


FIGURE 20.—Oxygen Concentration Gradient Over Length of Zirconium Rod After Heating By Direct Current to 1800° C. for 240 Hours.

Since this process is of the nature of a diffusion process, it was assumed that this curve should be of the form $y = Ce^{-nx}$ following that of a diffusion distribution function. It was found that the portion of the curve for x greater than unity followed this general form of the equation but that for values of x less than unity a marked deviation occurred. This can be explained by realizing that in the region for x greater than unity the oxygen migration is caused primarily by the voltage potential across the specimen since, in this region, the oxygen concentration is initially uniform. Even after a test run of 240 hours the curve on Figure 20 shows only a very slight concentration gradient in this region. However, at values of x less than unity the concentration gradient is large and it is evident that diffusion due to this gradient must occur and is opposite to the diffusion due to the potential across the specimen. There is then the effect of two opposing rates of diffusion in this latter region and thus may occur the deviation of the experimental curve from the above general form of the diffusion equation.

Calculations to consider a material balance of oxygen in the specimens is given in Appendix II. These calculations show that on the basis of the chemical analyses the number of oxygen atoms before and after the

test runs of 240 hours was 2.18×10^{20} atoms and 1.156×10^{20} atoms, respectively. This shows good agreement within the accuracy limits of the chemical analyses and the assumptions made for the simplification of the calculations. These calculations indicate that in the latter runs of this investigation very little contamination of the specimens had occurred.

In addition, if the diffusion coefficient for oxygen in zirconium were known, it would be possible to calculate not only the average mobility of the system but also the transport number according to the theories previously described. A thorough literature search revealed no such data for the oxygen-zirconium system were available. However, the diffusion coefficient for oxygen in zircaloy 2 has been determined by Mallett and his co-workers and can be used as an estimate for the oxygen-zirconium system (21, p. 181-185). The investigation of Mallett showed the diffusion coefficient for the oxygen-beta zirconium system to be 8×10^{-4} square centimeters per second. Using this value the mobility of oxygen in zirconium can be calculated from the equation

$$K = \frac{De}{kT}$$

or,

$$K = \frac{(8)(10)^{-4}(4.8)(10)^{-16}}{(300)(1.38)(10)^{-16}(2073)} = 4.47 \times 10^{-5} \text{ cm}^2/\text{sec-volt}.$$

This result shows a rather low value for the mobility which is reasonable considering the length of time required to cause the oxygen atoms to migrate to the anode end of the specimen during the test.

The transport number related to a specific system is an indication of the number of gram-atoms of a component in the system which are transported by one Faraday and according to the theory previously described may be written as

$$t_i = \frac{D_i C_i F (Z_i - z_i) e E}{k T f J} .$$

The term f is the correlation factor for diffusion which takes into account the various possibilities of ion movement through an interstitial lattice. The determination of this factor has been accomplished by Compaan and Haven for various crystal lattices by translating the problem of diffusion into the theory of electrical networks (7, p. 786-801). Their value for the correlation factor for the zirconium lattice is 0.78146 and will be used in the determination of the transport number for oxygen through zirconium. In addition, the calculations shown below are given for the specific conditions under

which this investigation was carried out, that is, a 0.125 inch diameter zirconium rod heated by a direct current of 120 amperes at 5 volt potential to a temperature of 1800 C. The effective length of this rod was 20.3 centimeters and the diffusion constant used will be 8×10^{-4} square centimeters per second. The approximate values of the terms used in the derived transport number equation give the following. Using the conditions under which the test was run the following terms are found.

$$D = 8 \times 10^{-4} \text{ cm}^2/\text{sec}$$

$$C_i = 4.08 \times 10^{-4} \text{ gram atom/cm}^3$$

$$F = 96,540 \text{ coulomb/gram equivalent}$$

$$(Z_i - z_i) = 2 \text{ gram equivalent/gram atom}$$

$$e = 4.8 \times 10^{-10} \text{ esu}$$

$$E = 8.2 \times 10^{-4} \text{ stat volt/cm}$$

$$k = 1.38 \times 10^{-16} \text{ erg/K}$$

$$T = 2073 \text{ K}$$

$$f = 0.78146$$

$$J = 1515 \text{ coulomb/sec cm}^2$$

Therefore,

$$t_i = \frac{(8)(10)^{-4}(4.08)(10)^{-4}(9.654)(10)^4(2)(4.8)(10)^{-10}}{(1.38)(10)^{-16}(2.073)(10)^3(0.78146)}$$

$$\frac{(8.2)(10)^{-4}}{(1.515)(10)^3}$$

or,

$$t_1 = 3.662 \times 10^{-5} \text{ gram-atoms/Faraday.}$$

This is then the number of gram atoms of oxygen which is transported per Faraday toward the anode end of the specimen during the course of the test. As before, in the calculation of the mobility, this is a relatively small number and was expected due to the long length of time required to show the effects of the solid state electrolysis.

In considering the earlier experimental results of this investigation, it is evident that although a marked increase of oxygen content is evident at the anode end of the rod, little if any decrease in oxygen content was accomplished as compared to the initial impurity level. It is believed that this was primarily due to the contamination of the specimen from leaks in the vacuum system. Several attempts at preventing this contamination by means of gettering shields to physically protect the zirconium were made. Finally, new vacuum seals and a complete reassembly of the base plate of the vacuum resulted in a low leak rate system which resulted in a lower impurity level. It might be mentioned here that other methods, such as placing an envelope of inert gas (argon) around the bell jar and base plate of

the system, were tried in order to investigate the possibility of lowering the amount of contamination in the zirconium. These methods produced no significant results.

Calculations were made to obtain an estimate of the amount of possible contamination assuming a reasonable leak rate into the system. Basic considerations of kinetic theory were used. It was found that for over a period of 240 hours sufficient oxygen could have been admitted into the system to cause the contamination showed by the chemical analysis. See Appendix I.

Resistivity measurements were made on some specimens in order to correlate on a qualitative basis the resistivity of zirconium as a function of its oxygen content. The results show that where there was a significant difference in oxygen content, there was a corresponding difference in resistivity, that is, a higher resistivity for a higher oxygen content. It was also noticed that after about 100 hours of testing a high temperature region appeared at the anode indicating a higher resistance in that region.

In addition to resistivity measurements, attempts were made to relate the zirconium hexagonal close-packed lattice parameter measurements to the oxygen content. Since oxygen occurs in the lattice as an interstitial,

an increase in oxygen content should produce a variation in the lattice parameter. It has been determined by Treco (20, p. 366) that the a_0 and c_0 dimensions for alpha zirconium both vary linearly and in the same proportion with the content of oxygen. This work was carried to only 2.5 atomic percent oxygen and showed that since both varied in the same proportion their ratio c/a would remain constant. It was therefore thought that if data could be found at the lower levels of oxygen content, an extrapolation could be made, and thus a method of estimating the oxygen content of the zirconium could be obtained.

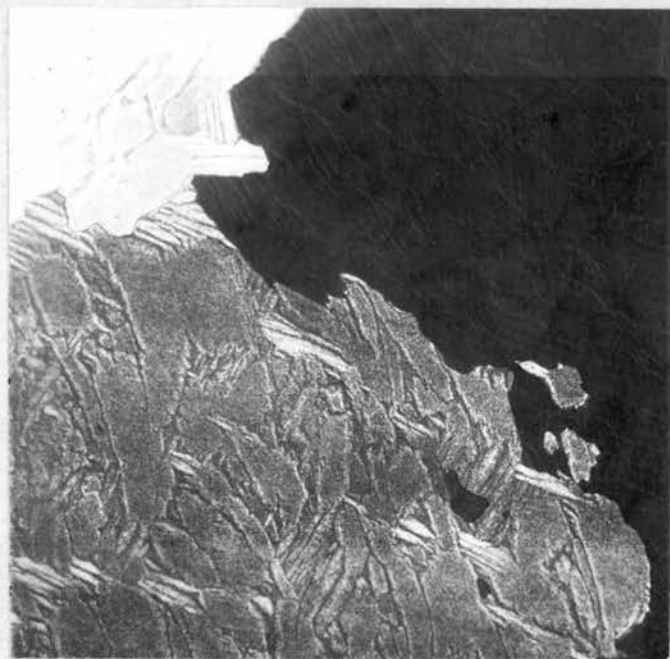
Lattice parameter measurements were attempted using specimens of known oxygen content from 300 ppm to 1300 ppm. A Norelco high precision back reflection lattice parameter measuring camera was used in this investigation. However, because of the highly oriented grains of the material, no precise measurements could be made.

The effects of oxygen migration was also seen through metallographic studies of the material tested. The alpha crystals formed by transformation from the beta phase often show complicated microstructures which varies greatly with the impurity content. It has been found that this is due to the way in which the alpha crystals

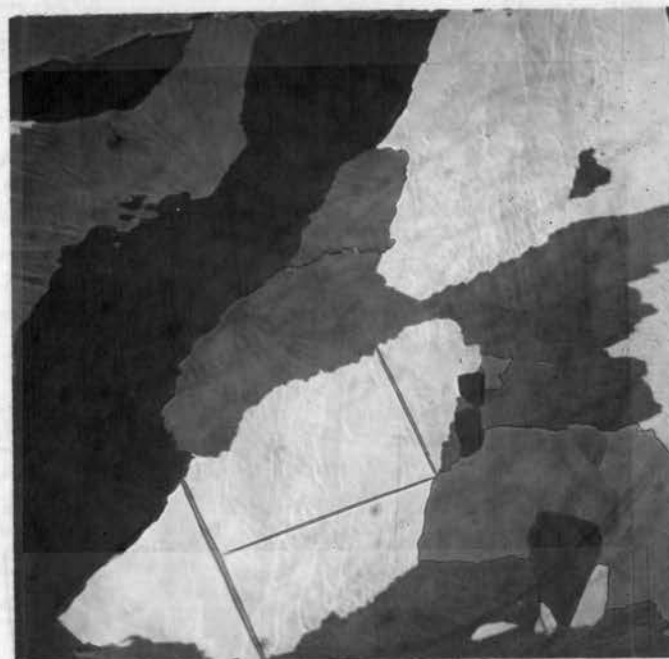
form in transforming from the beta phase, i.e., into oriented platelets instead of randomized equiaxed grains (20, p. 380). These impurities will cause a Widmanstatten structure in the material and can give a qualitative estimate as to the relative amounts of impurity levels present in the material.

Figure 21 shows the photomicrograph of a zirconium rod run at a three volt potential for periods of time of 70 and 213 hours. Both structures show little if any Widmanstatten structure but do show grain boundaries with a feathered appearance indicating some impurity effect and a relatively rapid cooling rate. The specimen run for 213 hours has considerably larger grain size. There is, however, little difference in their appearance which indicates no migration of oxygen. This is substantiated by chemical analysis which showed about 500 ppm oxygen content in each specimen.

With specimens run at a four volt potential the situation is not the same. This is shown in Figure 22. After a period of 24 hours the structure is similar to the case of the three volt potential exhibiting little Widmanstatten structure and feathery grains. After a period of 110 hours the microstructure is much different. This microstructure is dominated with an acicular and Widmanstatten structure indicating a great deal more



(a) 213 hours



(b) 70 hours

FIGURE 21. -- Photomicrographs Showing Microstructures of Zirconium Rods Being Held at 1800 C at 3 Volt Potential for (a) 213 Hours and (b) 70 Hours. Polarized light, B etch, 250X.

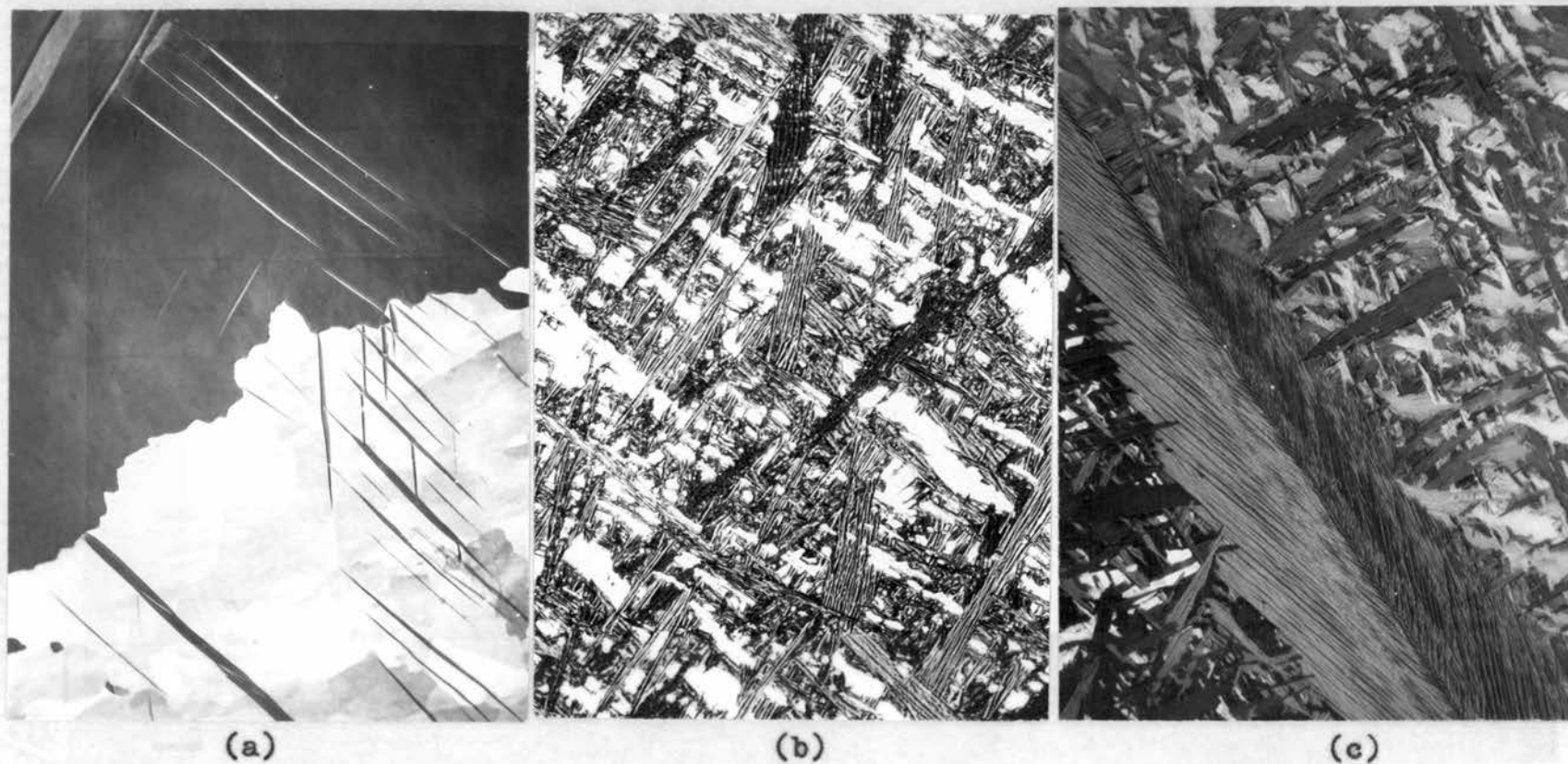


FIGURE 22. -- Photomicrographs Showing Microstructure of Zirconium Rods After Being Held at 1800 C at 4 Volts Potential for (a) 24 Hours, (b) 110 hours, and (c) 200 Hours. Polarized light, B etch, 250X.

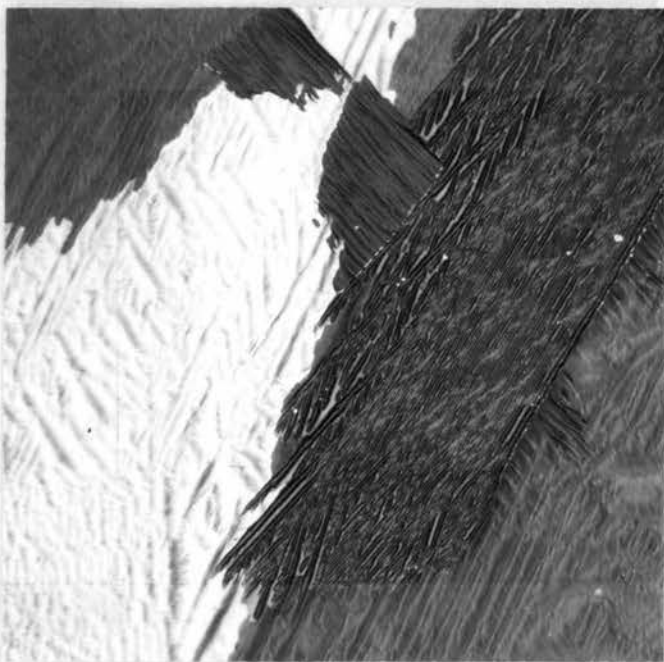
migration of oxygen. The same is true for the specimen run for 200 hours. In addition, the retained beta grain boundary is evident and indicated a great amount of impurity located in and around the grain boundary. These results were again substantiated by chemical analysis, the oxygen content being found to increase at the anode with increasing time. For 24, 110, and 200 hour runs at four volt potential the oxygen content was found to be 280, 810, and 2720 ppm, respectively.

Figure 23 can be compared to Figures 21a and 22c to see the effective difference in microstructure of material run for approximately the same interval of time but at three, four, and five volt potentials. This difference is again the variation in the amounts of Widmanstatten structure which increased with the increased amount of oxygen in the specimens.

Finally, Figure 24 shows the effective difference in microstructure along the length of a rod. It is evident that there is a large increase in impurity content as one compared the microstructure of the mid-section of the rod to that at the anode. The mid-section of the rod exhibits large grains containing some Widmanstatten structure and feathery grain boundaries while at the anode there is little indication of grain boundaries left, the entire field being in the form of fine Widmanstatten.



FIGURE 23. -- Photomicrograph Showing Microstructure of Zirconium Rod Held at 1800 C for 240 Hours at 5 Volt Potential. This may be compared to Figures 21a and 22c which were at 3 and 4 volt potentials, respectively. Polarized light, B etch, 250X.



(a) Mid-section



(b) Anode

FIGURE 24. -- Photomicrographs of a Zirconium Rod Held at 1800 C for 240 Hours Illustrating the Difference in Microstructure due to the Relative Oxygen Content at the Mid-section and Anode of the Rod. Polarized light, B etch, 250X.

Chemical analysis for the oxygen content of the mid-section and the anode were 1140 and 36,000 ppm, respectively.

CONCLUSIONS

The results of this investigation show conclusively that further purification of zirconium can be obtained through the processes of zone refining and solid state electrolysis. Use of such material in the determination of physical properties, phase diagrams of alloy systems, and studies in the solid state should prove useful in obtaining more accurate and reproducible results.

In purification by zone refining the ultimate purity was obtained by passing a molten zone over the rod three times at a rate of $2\frac{1}{2}$ inches per hour. In this case the impurity levels of Fe, Ni, Cu, and Al were 1 ppm, 2 ppm, 0.05 ppm, and 1 ppm, respectively. Comparison of these values with the initial impurity levels given in Table I indicates that the effect of the purification process is considerable. These values are by no means the ultimate obtainable. Further purification could be obtained by cropping the contaminated ends of the specimen and repeating the zone refining process.

The data presented indicate that more purification by zone refining took place when the rods were subjected to the slower rates of travel and for multiple passes over the rods. This is in accordance with the theory of

zone refining and is what would be expected since time is required for the impurities to diffuse through the melt and segregate. Also, since the process can be repeated many times, the impurity level must drop with an increase in the number of passes over the specimen. It was due to the lack of time for segregation at the higher rates of travel which caused some unpredictable results from chemical analysis.

The oxygen content of rods subjected to the effects of solid state electrolysis was reduced from 1100 ppm to a minimum of 190 ppm. Again, further purification could be obtained by either extending the time of the test or by cropping the end of the specimen and repeating the purification procedure.

The migration of oxygen was shown conclusively by chemical analysis, metallographic examination, and by the observation of the mechanical properties of the material after purification by solid state electrolysis. Further proof of this migration was accomplished by reversing the polarity of the potential across the specimen and finding that the increase of oxygen content had occurred at the opposite end of the rod.

The theoretical considerations in this investigation were limited in two important ways. First, in

the derivation of the transport number describing the parameters in the migration of oxygen through the zirconium lattice, it was shown how the transport number was dependent upon the diffusion coefficient of the oxygen-zirconium system. A complete survey of the literature showed that this constant has not been found for this system but had been found for the oxygen-zircaloy 2 system. Using these data as an approximation, the mobility and transport number for the oxygen-zirconium system was found to be $4.47 \times 10^{-5} \text{ cm}^2/\text{sec-volt}$ and $3.662 \times 10^{-5} \text{ gram-atoms/Faraday}$, respectively.

Second, in the case of zone refining, the theoretical derivations presented, following those made by Lord, did not take into consideration the amount of material lost due to vaporization. Consideration of the vapor pressures of iron, nickel, copper, and aluminum shows that this loss is considerable.

From the data presented, it may be concluded that in the case of purification of zirconium by solid state electrolysis the amount of oxygen removed is definitely a function of the voltage potential across the specimen and of the length of time exposed to the temperature and potential. It may be reasoned that it would also be a function of the temperature but this parameter was not determined in this investigation. It was found that the

amount of oxygen migrating increased with an increase in potential and with the amount of time of the test. It was also found that no migration was achieved at a potential of three volts or less but that this migration began at a potential of four volts.

Severe contamination of the zirconium was found in the earlier test runs in the course of this study. A small leak in the vacuum system could cause this contamination since the specimen was held at a high temperature for a long period of time. Calculations showed that a leak rate as low as 10 micron-liters per second permitted the absorption of many parts of oxygen into the zirconium.

RECOMMENDATIONS

It was previously mentioned that the diffusion coefficient for the oxygen-zirconium system has not been determined. It is then recommended that this coefficient be determined in order that the data found in this investigation be of greater value. Methods of determining this constant are varied and numerous. One practical method is with the use of isotopic tracers such as O^{18} introduced into the zirconium. Equipment used in this study, or equipment of similar nature, could be used in such determinations. Final analysis could most effectively be made by use of a mass spectrometer to determine the number of oxygen atoms crossing a plane of reference in a given time.

It is also recommended that further studies should take place in a vacuum system composed of glass parts throughout and that a vacuum better than 1×10^{-6} mm of Hg be used. By this means a cleaner system could be maintained and more accurate results thus obtained.

The most effective means of purifying the zirconium rods by zone refining was at the slowest rates of travel obtainable with the equipment used in this investigation. This indicates that a more efficient means of purifying might be obtained at even slower rates of

travel. Equipment should then be made and this point of the investigation carried further.

BIBLIOGRAPHY

1. Berzelius, J. Zirconium obtained by reduction of potassium zirconium fluoride. *Annalen der Physik* 4:121-127. 1825.
2. Birchenall, C. C. and R. F. Mehl. Self diffusion in alpha and gamma iron. *Journal of Metals* 2: 144-149. 1950.
3. Burns, L. Contributions to mathematics of zone refining. *Journal of Metals* 7:1017-1023. 1955.
4. Burton, J. A. et al. The distribution of solute in crystals grown from the melt. I. Theoretical. *Journal of Chemical Physics* 21:1987-1991. 1953.
5. Claisse, F. and H. P. Koenig. Thermal and forced diffusion of oxygen in beta titanium. *Acta Metallurgia* 4:650-654. 1956.
6. Cobine, J. D. Gaseous conductors, theory and engineering applications. New York, Dover Publications, 1958. 606 p.
7. Compaan, K. and Y. Haven. Correlation factors for diffusion in solids. *Transactions of the Faraday Society* 52:786-801. 1956.
8. Darken, L. S. and R. W. Gurry. Physical chemistry of metals. New York, McGraw-Hill, 1953. 535 p.
- ✓ 9. Davies, M. et al. Floating zone melting of solids by electron bombardment. *Journal of Applied Physics* 27:195-196. 1956.
10. Dayal, P. and L. S. Darken. Migration of carbon in steel under the influence of direct current. *Transactions of the American Institute of Metallurgical Engineers* 188:1156-1167. 1950.
11. deBoer, J. H. and J. D. Fast. Electrolysis of solid solutions of oxygen in metallic zirconium. *Recueil des Travaux Chimiques* 59:161-167. 1940.
12. Goldman, M. Influence de la temperature sur la separation isotopique sous l'effect du courant continu dans le gallium fondu. *Academie des*

Sciences 1414:243-246. 1956.

13. Hartley, G. S. and J. Crank. Some fundamental definitions and concepts in diffusion processes. Transactions of the Faraday Society 45:801-807. 1948.
14. Heuman, T. Electrolytic transport in metallic solutions. The Physical Chemistry of Metallic Solutions and Intermetallic Compounds Symposium 1:182-193. 1960.
15. Hoffman, R. E. et al. Self diffusion in solid nickle. Journal of Metals 8:483-486. 1956.
16. Hondras, E. D. and A. J. W. Moore. The influence of an electrical potential gradient on the thermal etching of silver. Acta Metallurgica 8:751-757. 1960.
17. Jost, W. Diffusion in solids, liquids, and gases. New York, Academic Press, 1952. 558 p.
18. Kendall, L. F. et al. Reaction kinetics of zirconium and zircaloy 2 in dry air at elevated temperatures. Nuclear Science and Engineering 3:171-185. 1958.
- ✓ 19. Lord, N. W. Analysis of molten-zone refining. Journal of Metals 197:1531-1536. 1953.
20. Lustman, B. The metallurgy of zirconium. New York, McGraw-Hill, 1955. 776 p.
21. Mallett, M. W. et al. The diffusion of oxygen in alpha and beta zircaloy 2 and zircaloy 3 at high temperatures. Journal of Electrochemical Society 106:181-185. 1959.
22. Marzke, O. T. (ed.) Impurities and imperfections. Cleveland, American Society for Metals, 1955. 231 p.
23. Pfann, W. G. Zone melting. New York, Wiley, 1958. 236 p.
- ✓ 24. Pfann, W. G. and D. W. Hagelbarger. Electromagnetic suspension of a molten zone. Journal of Applied Physics 27:12-18. 1956.

25. Reiss, H. Mathematical methods for zone melting processes. American Institute of Mining and Metallurgical Engineers 200:1053-1059. 1954.
26. Seith, W. and H. Wever. Neue Ergebnisse bei der Elektrolyse fester metallischer Phasen. Zeitschrift fur Elektrochemie 59:942-946. 1955.
27. _____. Uber einen neuen Effect bei der elektrolytischen Uberfuehrung in festen Legierungen. Zeitschrift fur Elektrochemie 57: 891-900. 1953.
28. Skinner, G. B. et al. Vapor pressure of zirconium. Journal of American Chemical Society 73:174-176. 1951.
29. Smigelskas, A. D. and E. A. Kirkendahl. Zinc diffusion in alpha brass. Transactions of the American Institute of Mining and Metallurgical Engineers 171:130-137. 1947.
30. Wernick, J. H. Determination of diffusivities in liquid metals by means of temperature gradient zone melting. Journal of Chemical Physics 25: 47-49. 1956.
31. Wever, H. Electrolytic transport and conduction mechanism in iron and nickel. The Physical Chemistry of Metallic Solutions and Intermetallic Compounds Symposium 1:283-290. 1960.
32. _____. Uber fuehrungsversuche an festem Kupfer. Zeitschrift fur Electrochemie 60:1170-1175. 1956.
33. Williams, J. M. and E. L. Huffine. Solid state electrolysis in yttrium metal. Nuclear Science and Engineering 9:500-506. 1961.

APPENDIX

APPENDIX I

The following analysis is used to compute by means of basic kinetic theory the possible oxygen contamination to zirconium rods submitted to a temperature of 1800 C under a vacuum of 2×10^{-5} mm of Hg. It is assumed for the purpose of these calculations that the vacuum system has a leak rate of 10 micron liters per second and that it has a volume of 112.7 liters (11.27×10^4 cubic centimeters).

By the Gay-Lussac law we know that $pV = RT$ where RT has the units of energy. If we assume that n is the number of molecules per cubic centimeter in the system we can express this as the ratio N_0/V_0 where N_0 is the constant Avogadro's number and V_0 is the volume of a gram molecule of the gas. Therefore, we may write

$$P = \frac{RT}{V_0} = \frac{RnT}{N_0}$$

or,

$$P = nkT \text{ -----(1)}$$

where

$$k = 1.38 \times 10^{-16} \text{ ergs/K}$$

$$P = \text{dynes per square centimeter}$$

$$n = \text{molecules per cubic centimeter}$$

$$T = \text{absolute temperature, K.}$$

Assuming an operating pressure of 2×10^{-5} mm Hg and an environmental temperature of 400 K we may find the number of molecules per cubic centimeter by use of equation (1).

$$n = \frac{P}{kT} = \frac{(2)(10)^{-5}(1.33)(10)^3}{(1.38)(10)^{-16}(400)}$$

$$n = 4.82 \times 10^{11} \text{ molecules/cubic centimeter}$$

Assuming that this number of molecules is in the chamber at the start of the test run is in fact air, we may assume that one-fifth of this amount are oxygen molecules. Therefore,

$$n_o = \frac{2}{5} (4.82)(10)^{11} = 1.93 \times 10^{11} \text{ atoms/cc.}$$

For a volume of 112.7 liters, the total number of oxygen atoms in the system is then

$$n = (1.93)(10)^{11}(11.27)(10)^4 = 2.17 \times 10^{16} \text{ atoms.}$$

For the assumed leak rate of 10 micron liter per second, we calculate by similar means the number of oxygen atoms at 2×10^{-2} mm of Hg, the difference between this and the concentration at 2×10^{-5} mm Hg being the number of atoms entering per second of time into the system. Let this number at 2×10^{-2} mm Hg be denoted by n' . Therefore,

$$n' = \frac{(2)(10)^{-2}(1.33)(10)^3}{(1.38)(10)^{-16}(400)} = 4.82 \times 10^{14} \text{ molecules/cc}$$

Converting from air to oxygen atoms and assuming that the test run was for 240 hours (8.64×10^5 seconds), we can write for the total number of oxygen atoms entering the system during the test run,

$$n = \frac{2}{5} (4.82)(10)^{14}(1000)(8.64)(10)^5 \text{ atoms}$$

$$n = 1.67 \times 10^{23} \text{ atoms.}$$

The difference between this and the original number in the system being negligible, we can use this figure as an estimate of the number of oxygen atoms which have entered the system over a period of time of 240 hours. Converting this number into the possible atomic percent in the zirconium rod 10.5 grams in weight we obtain

Atomic percent Zr =

$$\begin{aligned} & \frac{\text{No. of oxygen atoms (100)}}{\text{No. of oxygen atoms} + \text{No. of zirconium atoms}} \\ &= \frac{(1.67)(10)^{23}(100)}{(1.67)(10)^{23} + (6.92)(10)^{22}} = 70.6 \text{ a/o} \end{aligned}$$

This number is of course much higher than the average concentration of oxygen found in the first specimens tested by solid state electrolysis. However,

since the specimen was surrounded by the heat shield it can be assumed that some oxygen was absorbed by the shield. Also, these calculations do not take into account the number of atoms swept away by the vacuum pumps. It is therefore reasonable to assume that in the initial stages of this investigation substantial contamination could have occurred.

APPENDIX II

Oxygen Material Balance

Chemical analysis of the zirconium rods makes possible the calculation of an oxygen material balance on the specimen before and after purification by solid state electrolysis. As shown in Figure 20, the initial oxygen content in the 10.5 gram specimen was 1100 ppm. To estimate the total number of oxygen atoms in the rod before and after purification, assume the distribution curve is formed from two straight line segments. It is possible then to calculate the number of oxygen atoms in the first $\frac{1}{2}$ inch (segment A) and the last $7\frac{1}{2}$ inch (segment B) of the rod assuming two linear distributions.

The number of oxygen atoms initially in the rod can be found using the chemical analysis which showed that the rod contained 1100 ppm of oxygen distributed uniformly along the rod. The weight of oxygen is then

$$(0.0011)(10.5) = 0.01155 \text{ grams}$$

or, the number of atoms of oxygen is

$$\frac{(0.01155)(6.023 \times 10)^{23}}{32} = 2.18 \times 10^{20} \text{ atoms.}$$

This should compare to the total number of oxygen atoms

in the two segments A and B as calculated below.

For segment A, assuming a linear distribution over the $\frac{1}{2}$ inch interval, the average oxygen content is 0.235% by weight. Therefore, the number of atoms of oxygen is

$$\frac{(0.5)(10.5)(6.023(10)^{23})}{(8)(32)} = 2.92 \times 10^{19} \text{ atoms.}$$

For segment B, assuming a linear distribution over the remaining $7\frac{1}{2}$ inches of the rod, the average oxygen content is 0.0515% by weight and the number of oxygen atoms in this segment is therefore,

$$\frac{(7.5)(10.5)(6.023(10)^{23})}{(8)(32)} = 9.54 \times 10^{19} \text{ atoms.}$$

The sum of the oxygen atoms in segments A and B is therefore estimated to be 1.156×10^{20} atoms of oxygen which compared favorably with the initial oxygen content of the specimen when one considers the assumptions made in the calculations and upon the accuracy of the measurements.